Topological Phases at Ferroelectric Oxide Interfaces

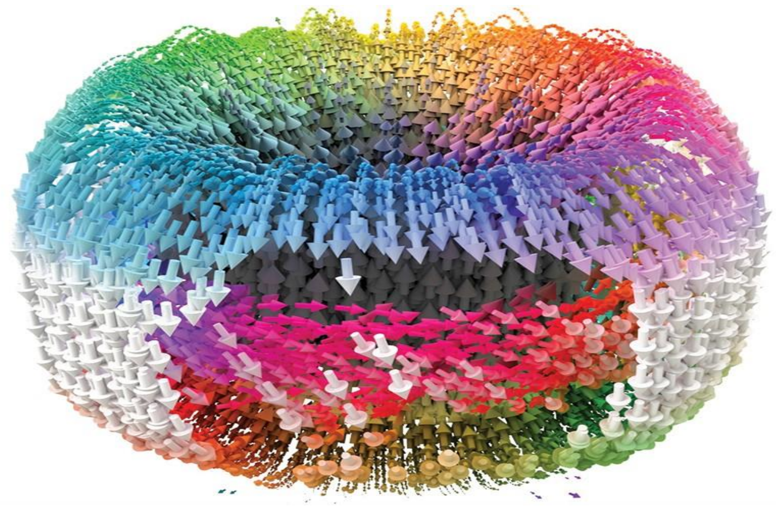

YRLGW: Correlation and topology in Magnetic materials

Fernando Gómez Ortiz

UNIVERSIDAD DE CANTABRIA

LIÈGE université

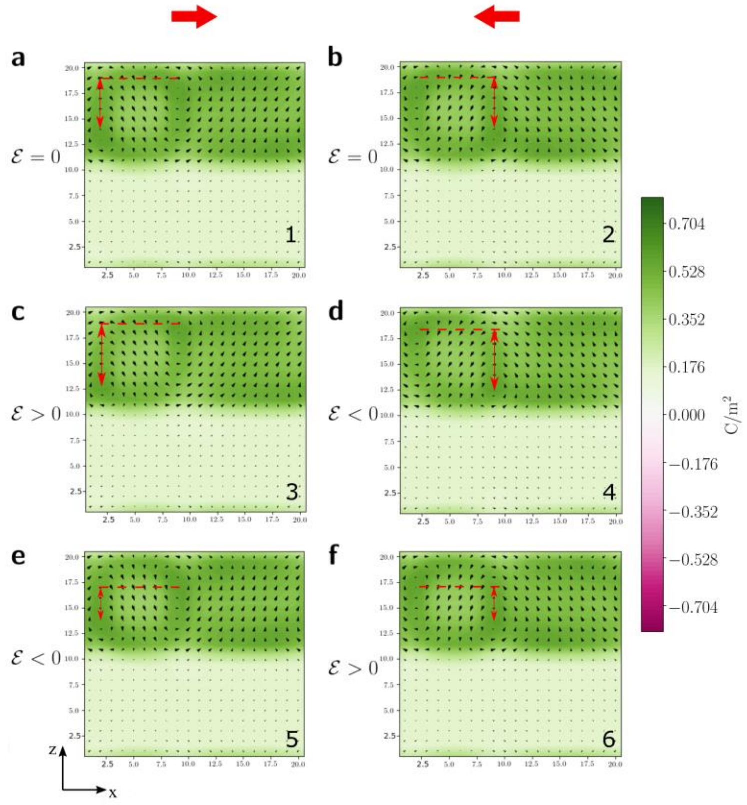

Mainz July 2024

Present some of the different polarization patterns exhibited by ferroelectric nanostructures and their functional properties

Theoretical/computational perspective

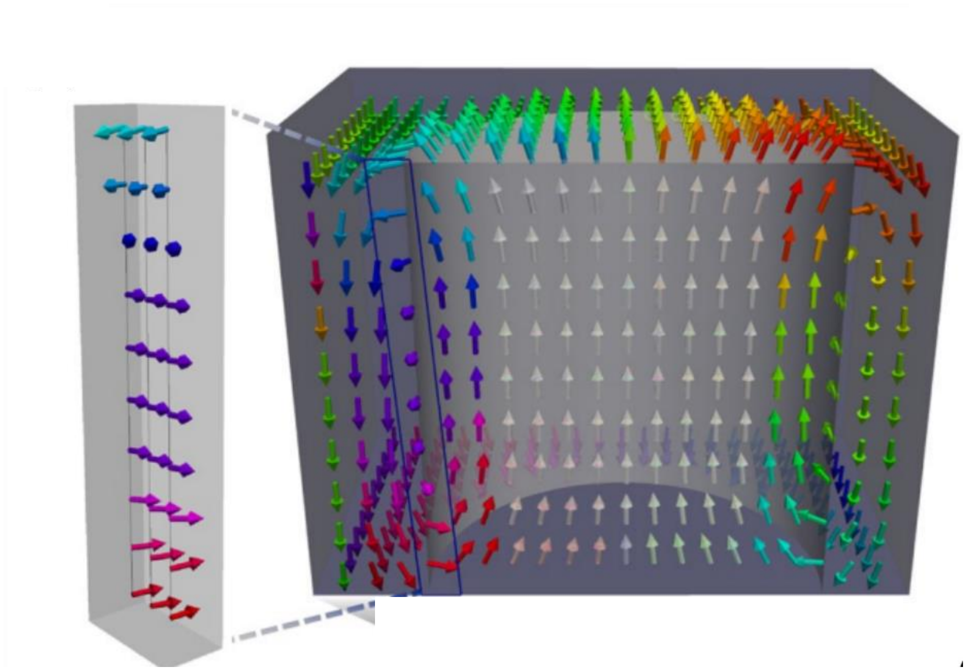

Prof. J. Junquera. PhD Advisor

Experimental perspective

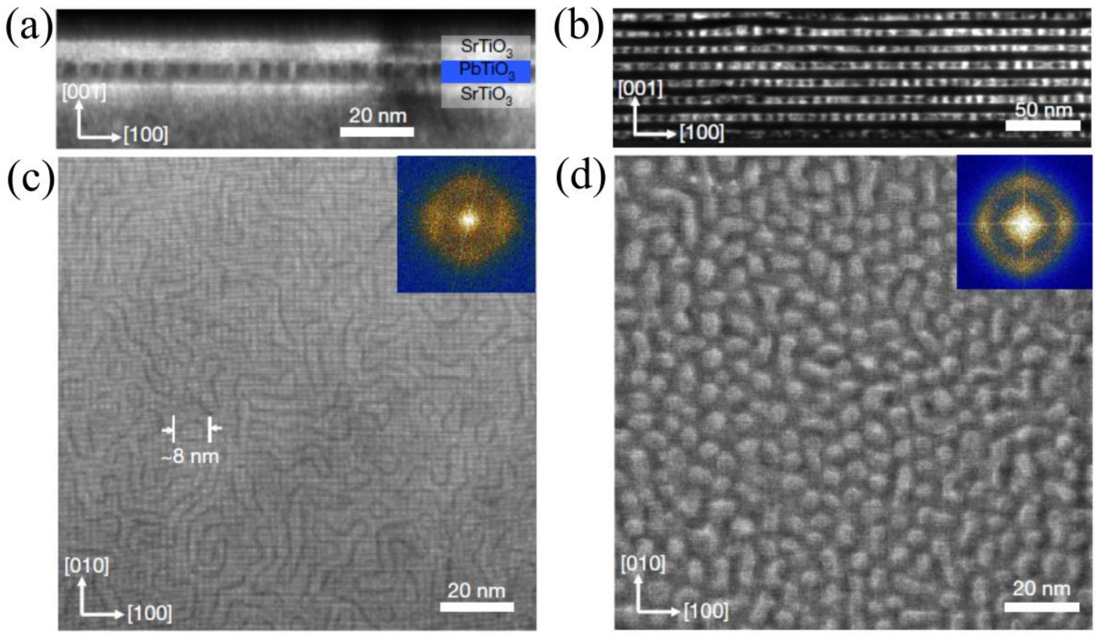

Close colaboration with the group of R. Ramesh at UC Berkeley during the thesis work

Topological phases in magnetic systems:

Interplay between **Exchange** and **Dzyaloshinskii-Moriya** interaction:

$$\mathcal{H}_{ij} = -J\overrightarrow{S_i}\cdot\overrightarrow{S_j} - \overrightarrow{D_{ij}}\,\overrightarrow{S_i}\times\overrightarrow{S_j}$$

Exchange

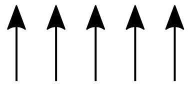

DMI

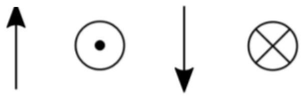

Interplay

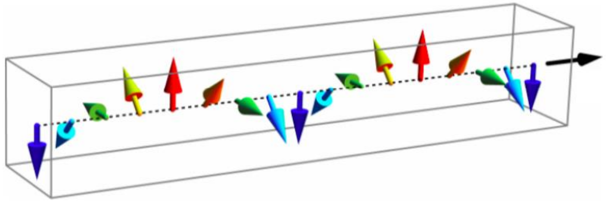

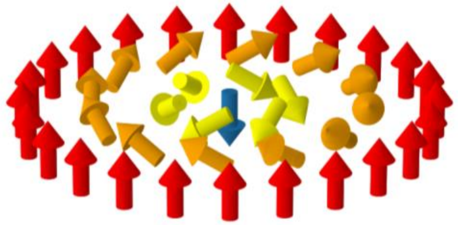

Bloch

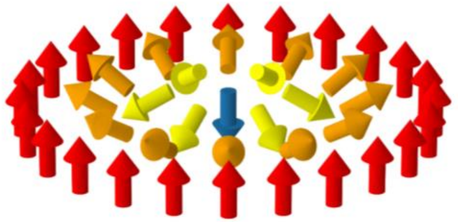

Néel

Predicted since 1990. Experimentally observed 2009

Applications in nanoelectronic industry… racetrack memories

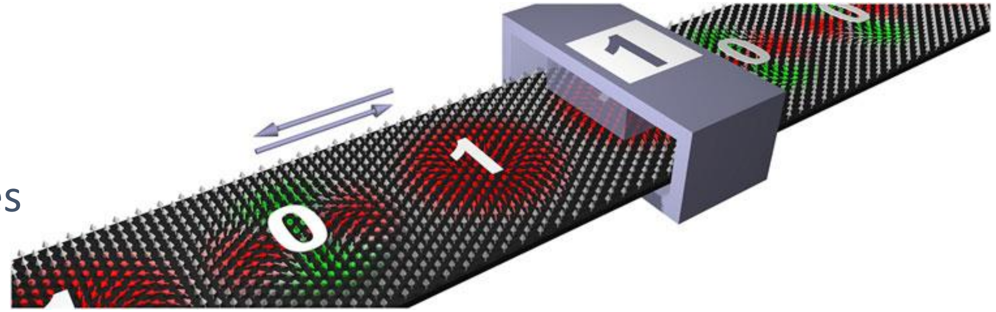

S. Parkin *et al.* Science, **320**, 190 (2008)

Can we encounter the same type of textures in ferroelectrics?

Many similitudes between Ferromagnets and Ferroelectrics

Similarities

-Existence of hysterisis loop

-Existence of domain structures

-Temperature driven phase tranision

Differences

-Apparently no DM analogue at that time.

-Polarization strongly coupled to lattice.
High elastic energy cost tilting dipoles.

-No need to form complex polarization textures
to accomodate competing interactions

In principle we should not expect them in ferroelectric structures

However… First and second principles calculations predict them

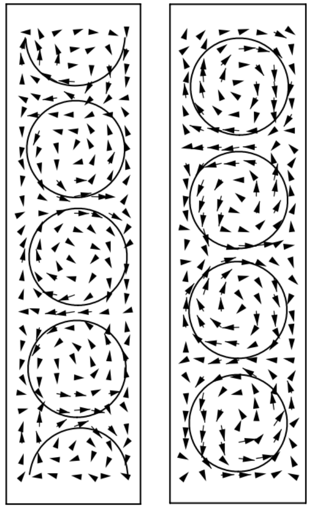

Vortices in ferroelectric nanostructures
Naumov *et al.* Nature **432**, 737 (2004)

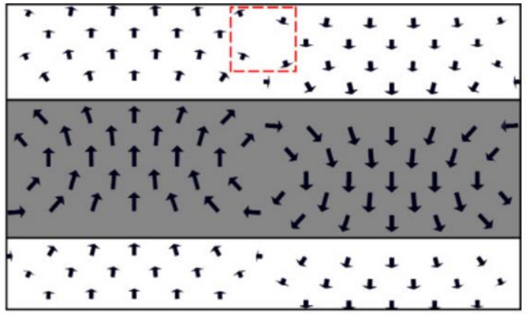

Vortices in PTO/STO superlattices
P. Aguado-Puente and J. Junquera
Phys. Rev. B **85**, 184105 (2012)

Importance of computational physics in material science

Multitude of fascinating and exotic properties boasted by transition metal oxides

ABO_3 perovskites oxides:
simple structure, wide variety of properties

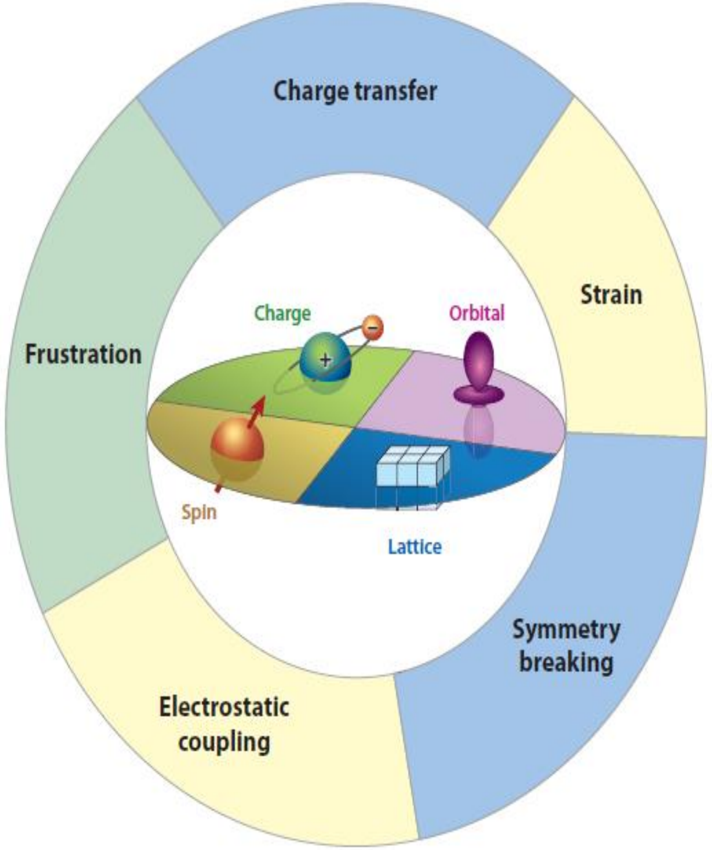

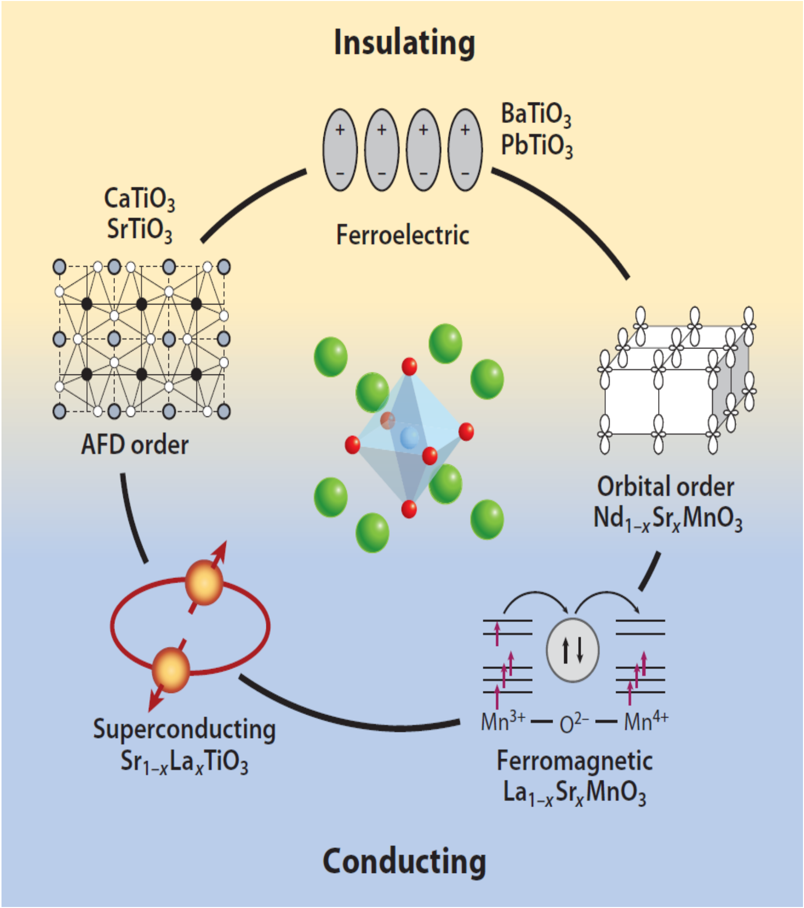

P. Zubko *et al*., Annu. Rev. Condens. Matter Phys. **2**, 141 (2011)

Ferroelectric Materials

The case of $PbTiO_3$

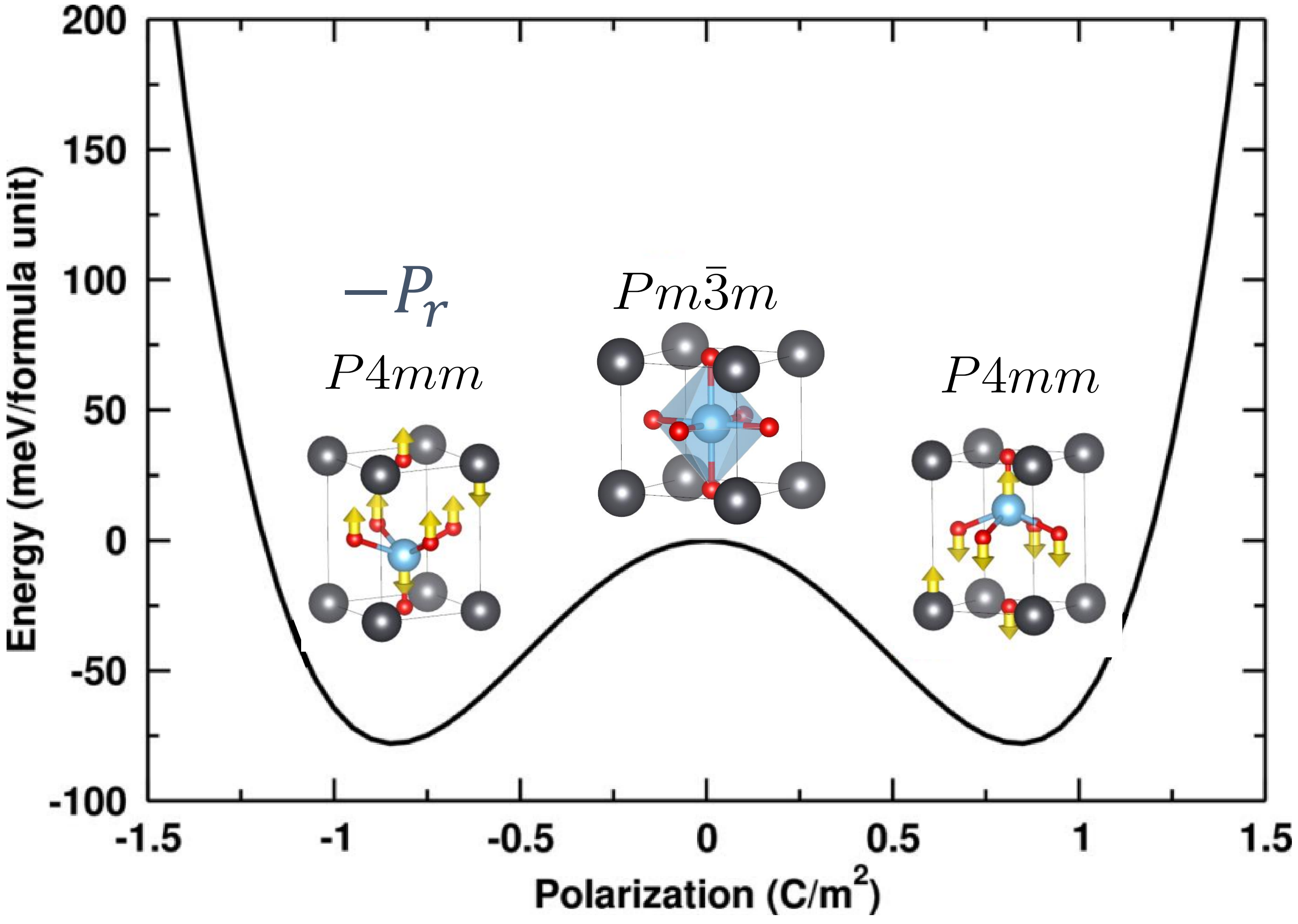

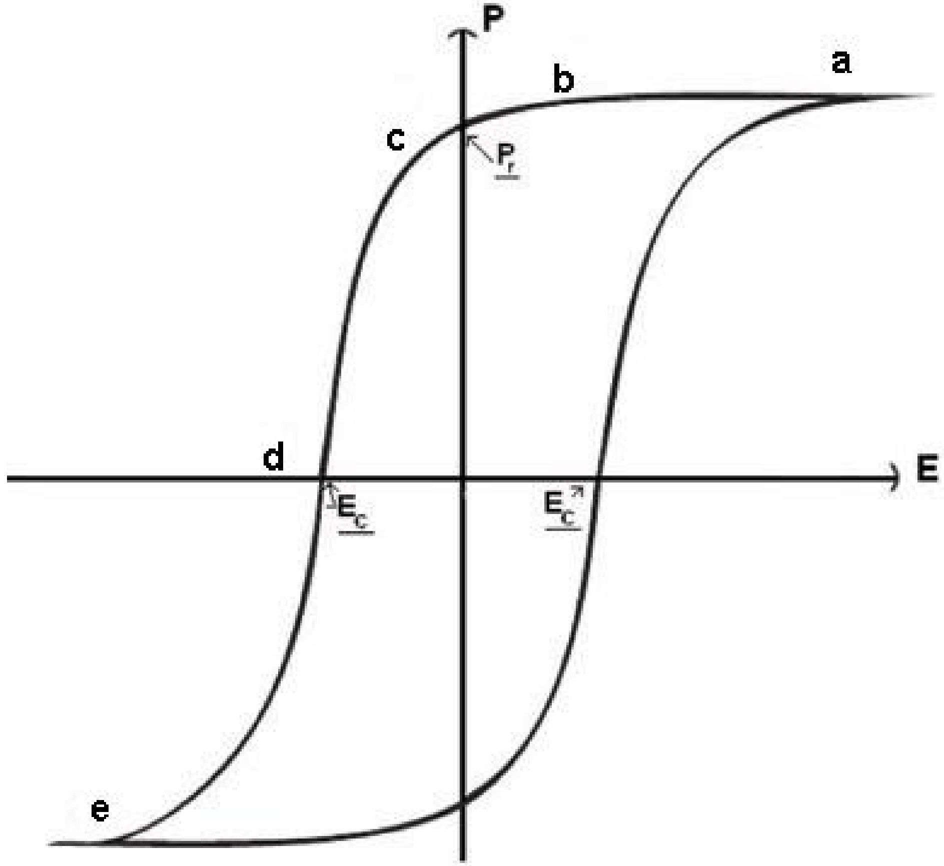

Paraelectric Materials

The case of $SrTiO_3$

There are other types of instabilities that lower the energy but preserve centrosymmetric character

High T, High symmetry Phase

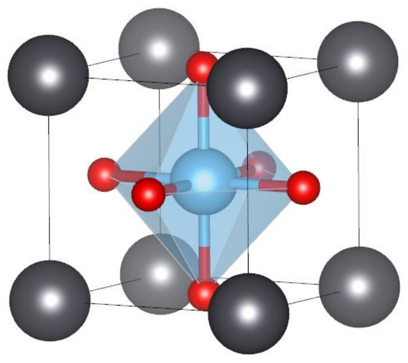

$Pm\bar{3}m$

Low T, Lower symmetry Phase

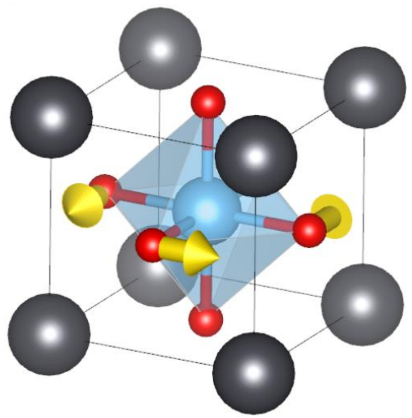

$I4/mcm$

Polar (ξ) and antiferrodistortive (ϕ) distortions usually present bi-quadratic coupling ($E \propto \xi^2\phi^2$) inhibiting their occurrence at the same time.

“The Interface is still the device”

Properties of A/B superlattice

$\neq$

Properties of A + Properties of B

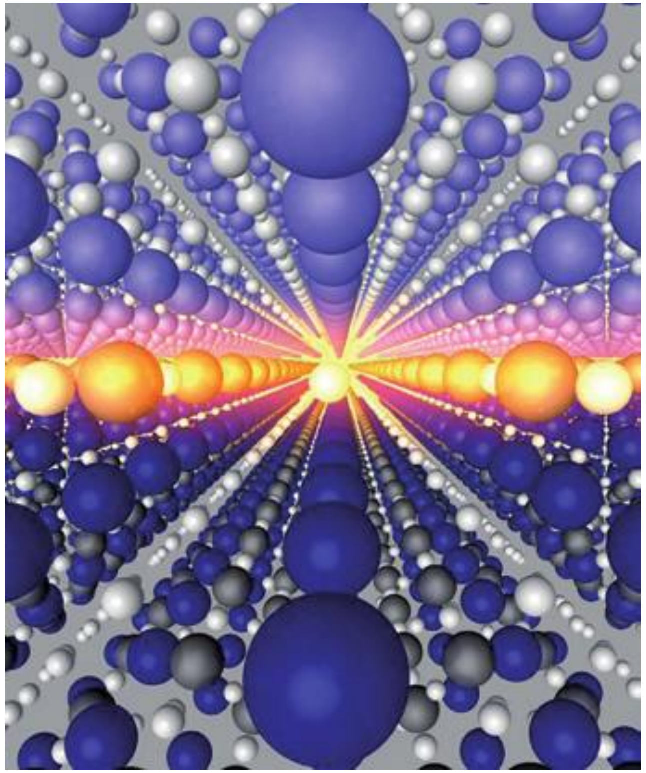

J.MANNHART (MPI-FKF) & A. HERRNBERGER (UNIV. AUGSBURG)

Editorial, Nature Materials **11**, 91 (2012)

A. Ohtomo and H. Y. Hwang, Nature **427**, 423 (2004)

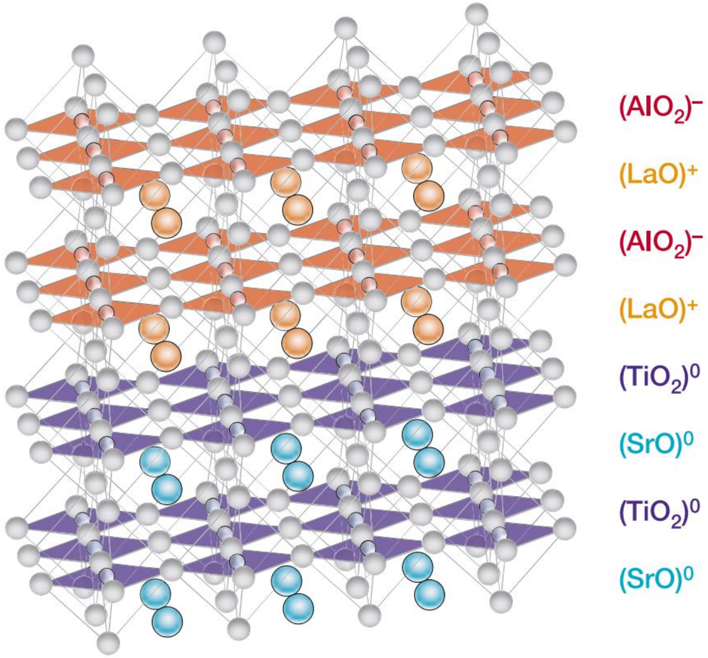

$LaAlO_3/SrTiO_3$ interface displays
High mobility 2D electron gas

E. Bousquet *et al.* Nature **452**, 732 (2003)

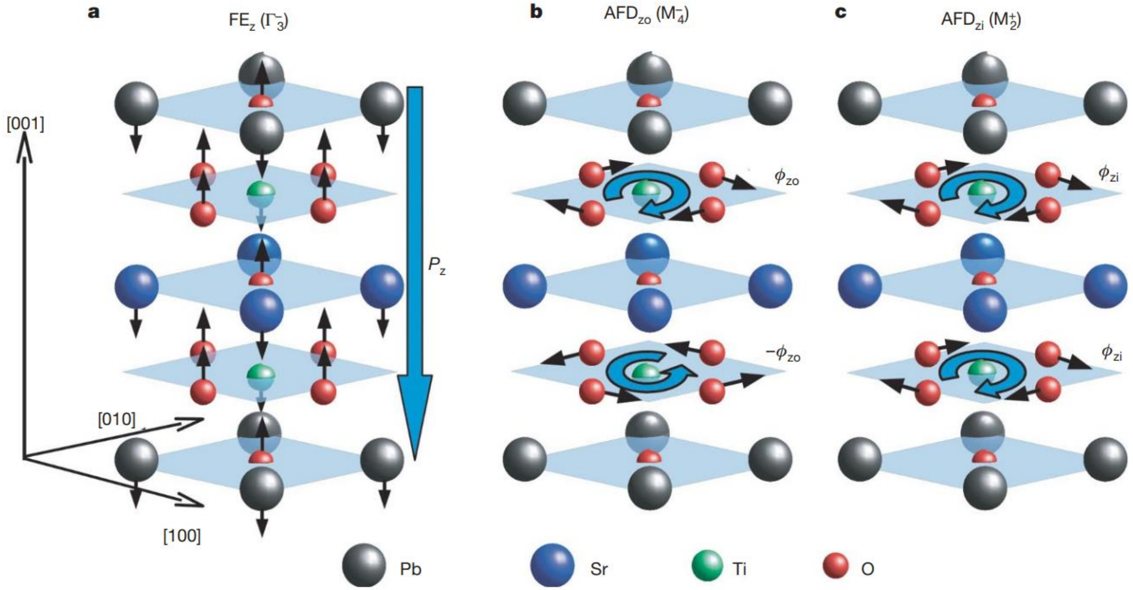

Improper ferroelectricity
in $PbTiO_3/SrTiO_3$ interface

$(PbTiO_3)_n/(SrTiO_3)_n$ superlattices

$PbTiO_3$ Uniaxial Ferroelectric. Strong polarization/strain coupling

$SrTiO_3$ Paraelectric material

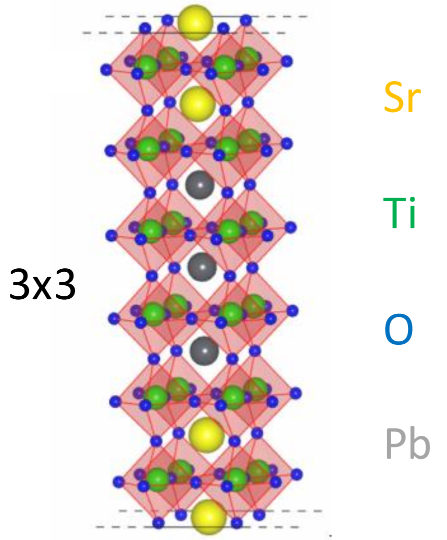

P. Aguado-Puente and J. Junquera PRB **85**, 184105 (2012)

…However, when combining them into a superlattice…
Elastic, **Electrostatic** and **Gradient** energies compete

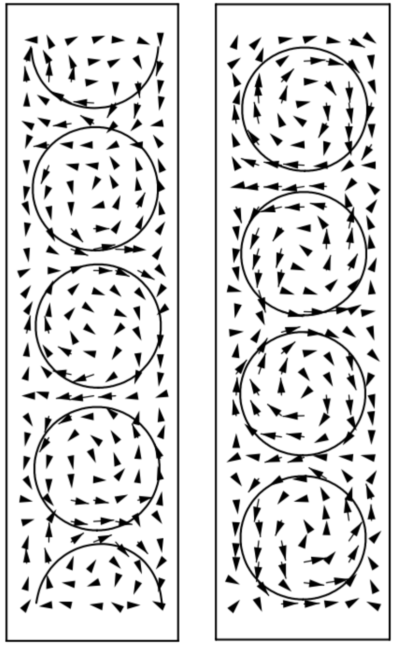

Vortices in ferroelectric nanostructures
Naumov *et al.* Nature **432**, 737 (2004)

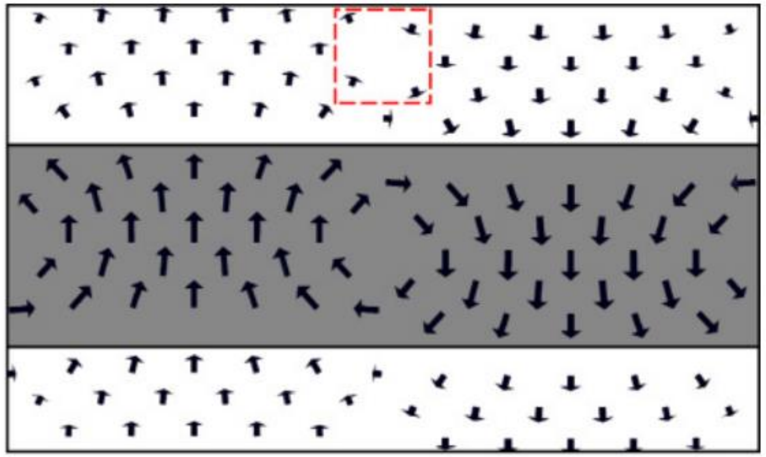

Vortices in PTO/STO superlattices
P. Aguado-Puente and J. Junquera PRB **85**, 184105 (2012)

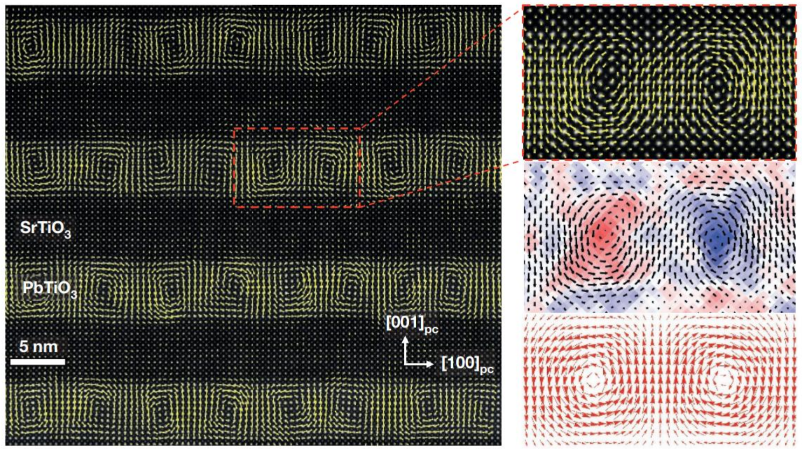

Vortices in PTO/STO superlattices
A. K. Yadav *et al.* Nature **530**, 198 (2016)

Physical ingredients to develop continuously rotating textures:

Free standing slab

Oppositely to bulk crystals, in slabs homogeneous polarization is precluded due to surface termination

$$\nabla \vec{P} = -\rho_b$$

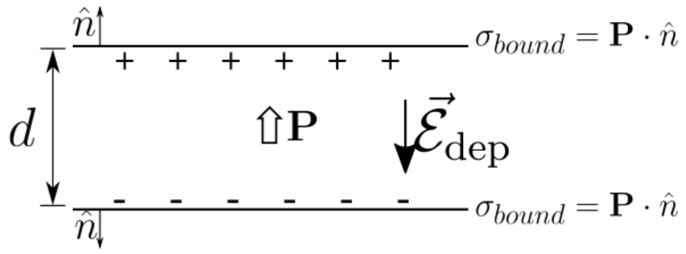

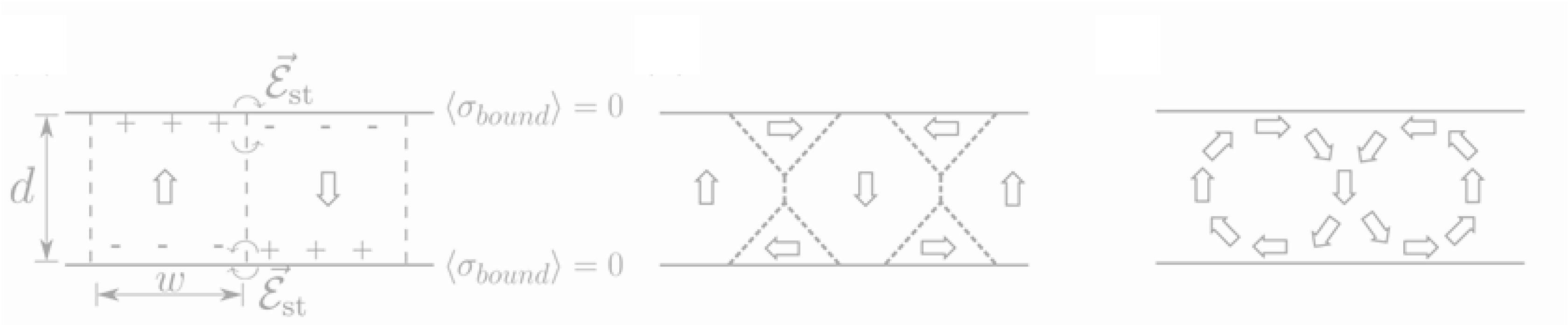

$$\mathcal{E}_{dep} = -\frac{1}{\epsilon_0} P$$
$$E \propto P^2$$

HUGE electrostatic penalty

Physical ingredients to develop continuously rotating textures:

Free standing slab

Domain formation achieve charge neutrality at the surfaces reducing enormously the electrostatic penalty

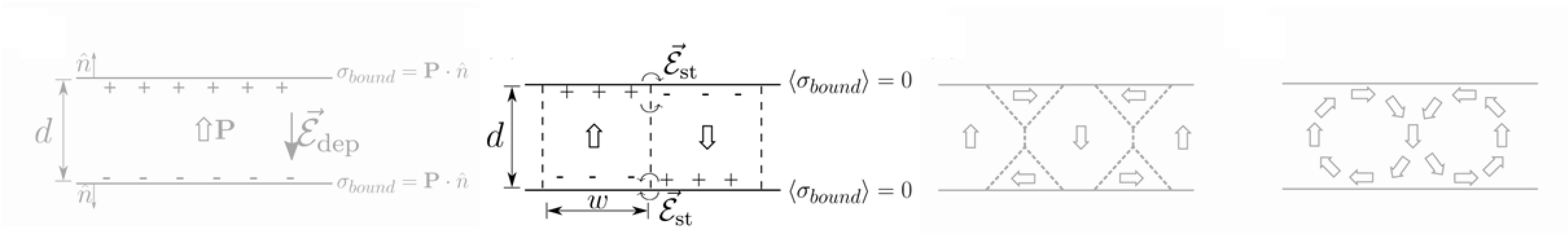

Generation of domains is associated with an energy cost due spatial gradient of $\vec{P}$

$$E \propto (\partial_x P_z)^2$$

The delicate balance between electrostatic and gradient terms determine the density of domains

$$\omega^2 \propto d$$

Kittel Law

Physical ingredients to develop continuously rotating textures:

Free standing slab

The presence of domains greatly relax the electrostatic energy.
However, stray fields are still large at the interfaces

Usually large enough to tilt the polarization

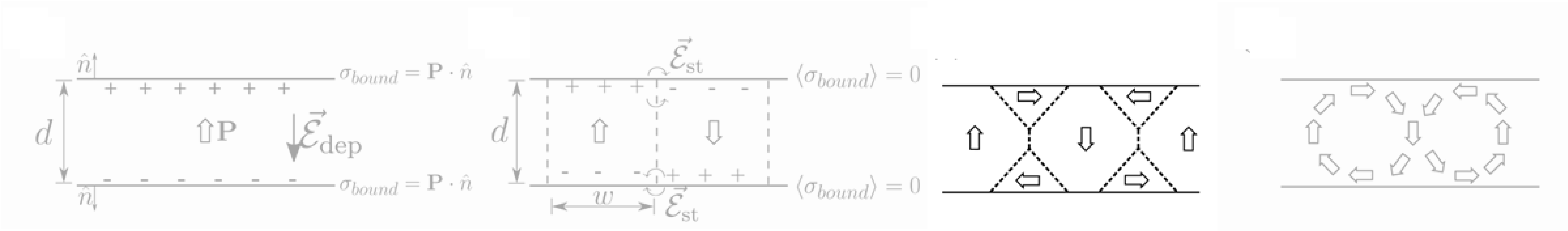

Balace between elastic energy of tilting the polarization and electrostatic relaxation

Flux-Closure domains

Physical ingredients to develop continuously rotating textures:

Free standing slab

Finally, the balance between elastic and gradient terms can relax 90º and 180º domains and transit to a continuously rotating texture

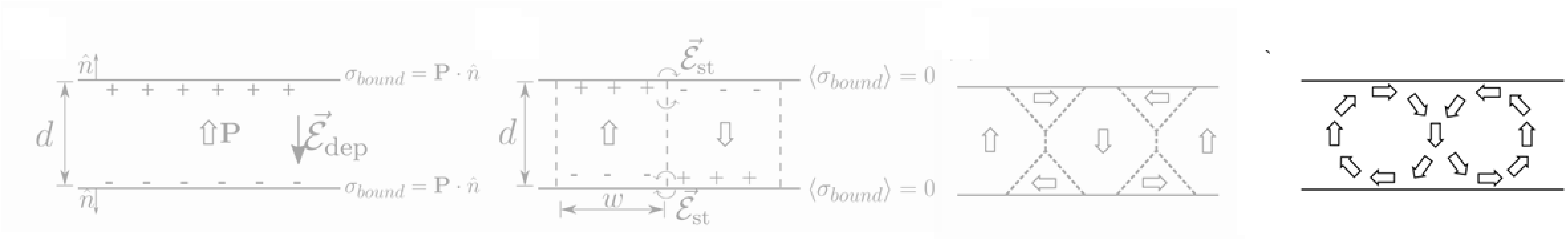

This can be tuned by means of

- Strain
- Thickness of ferroelectric material
- Electrostatic boundary conditions

First experimental observation of a Ferroelectric Skyrmion

Experimental realization

S. Das,…, F. Gómez-Ortiz et al. Nature **568**, 368 (2019)

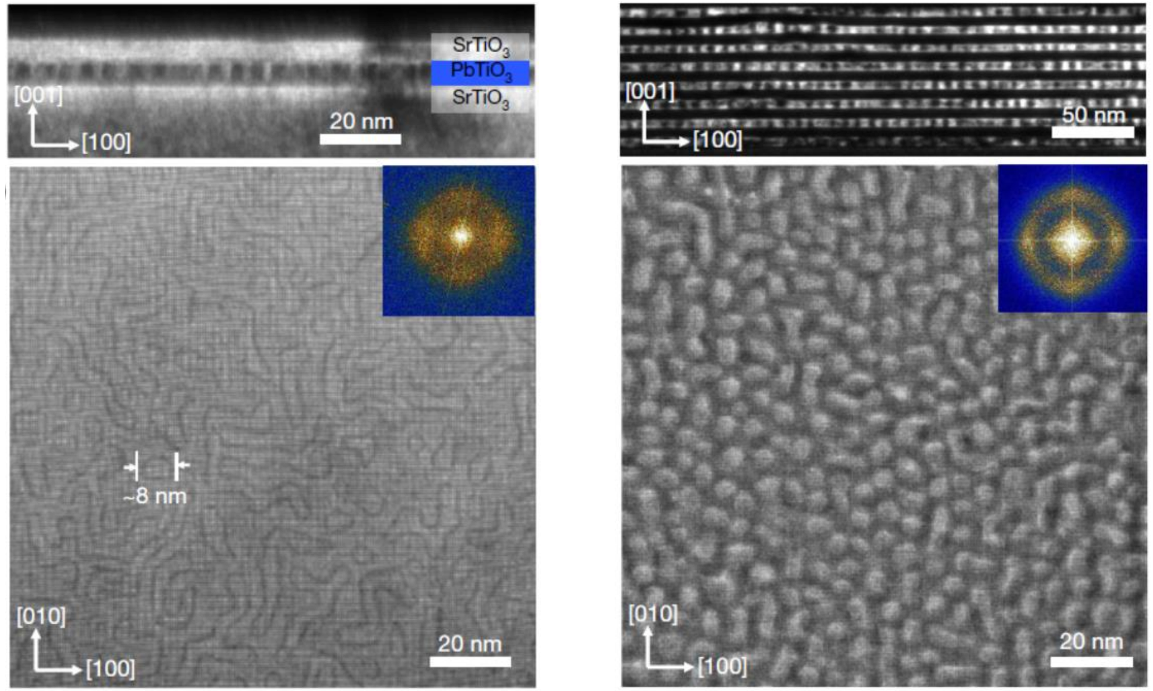

$[(PbTiO_3)_n/(SrTiO_3)_n]_m$ heterostructures, where n = 12 – 20 unit cells and m =1 – 8 repetitions.
Grown on TiO_2-terminated single-crystalline $SrTiO_3$

Theoretical stabilization

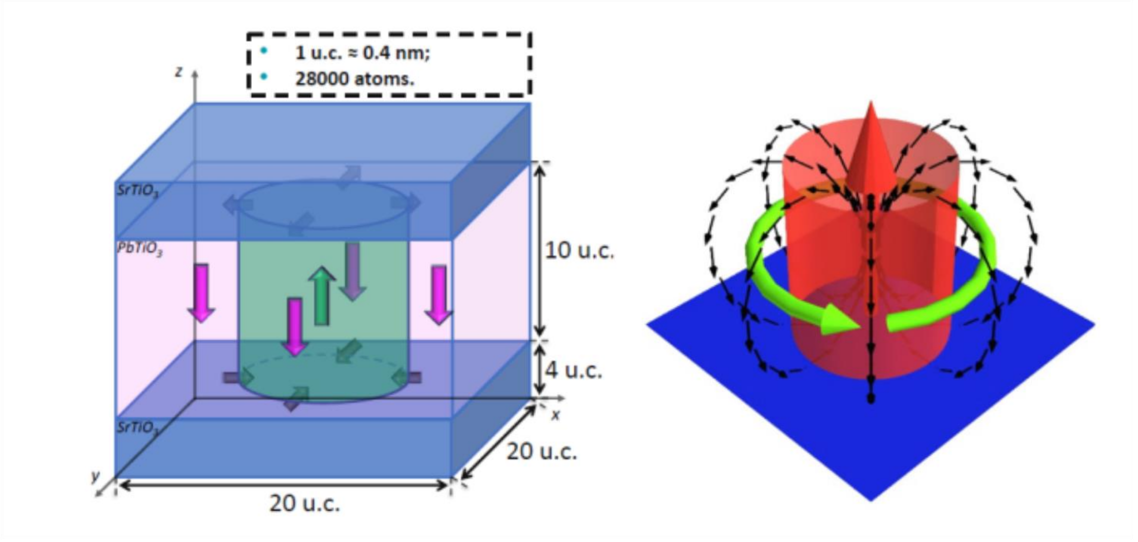

Core region of positive polarization embedded in a negative polarization matrix.

Bloch and Néel components develop after relaxation.

Observation of room temperature polar Skyrmions

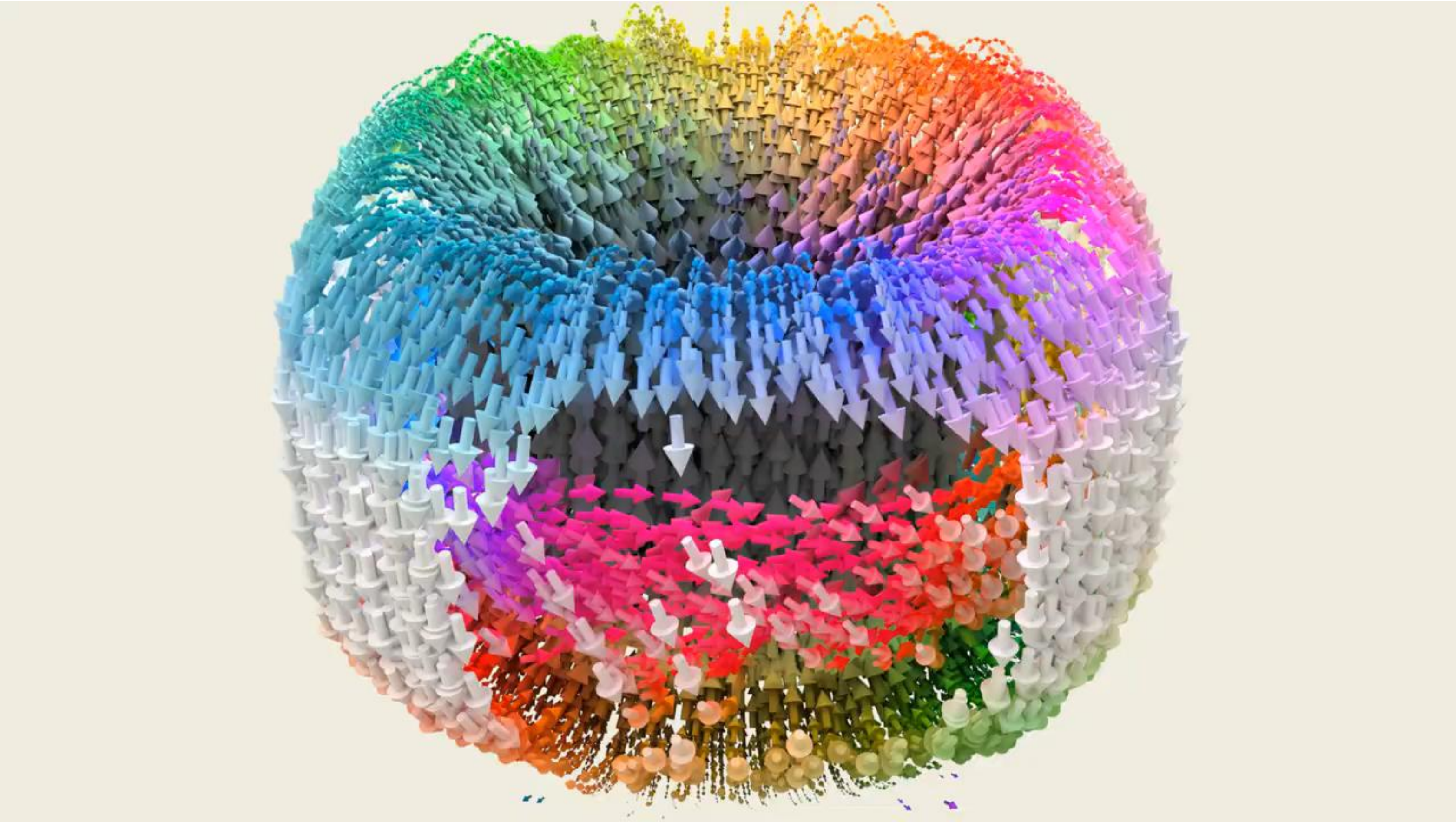

S. Das,…, F. Gómez-Ortiz *et al.* Nature 568, 368 (2019)

Inner core of positive polarization completeley surrounded by a negative matrix.

In between the polarization rotates continuously.

Topological Characterization of polar bubble Skyrmions

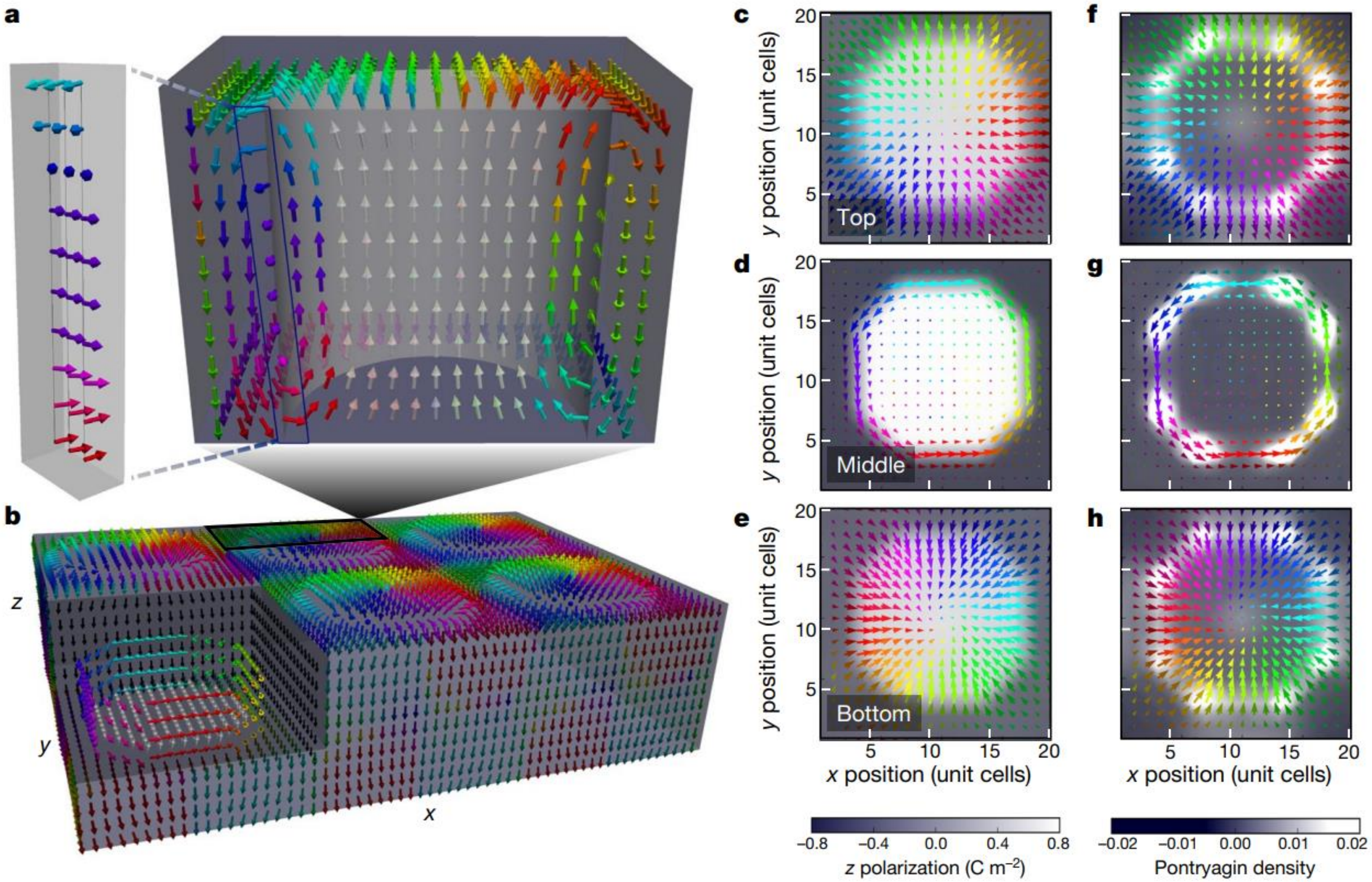

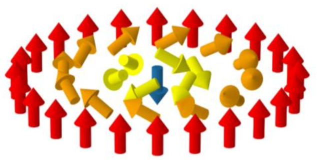

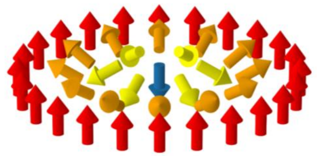

S. Das,…, F. Gómez-Ortiz *et al.* Nature 568, 368 (2019)

$$N_{Sk} = \frac{1}{4\pi} \int\int \vec{p} \cdot \left(\frac{\partial \vec{p}}{\partial x} \times \frac{\partial \vec{p}}{\partial y} \right) dxdy$$

Topological Characterization

Conserved skyrmion number plane by plane. $N_{Sk} = +1$.
Topological invariant. Similar to Magnetic counterparts, **smaller and tunable with $\mathcal{E}$**

Rich phase diagram of polar textures

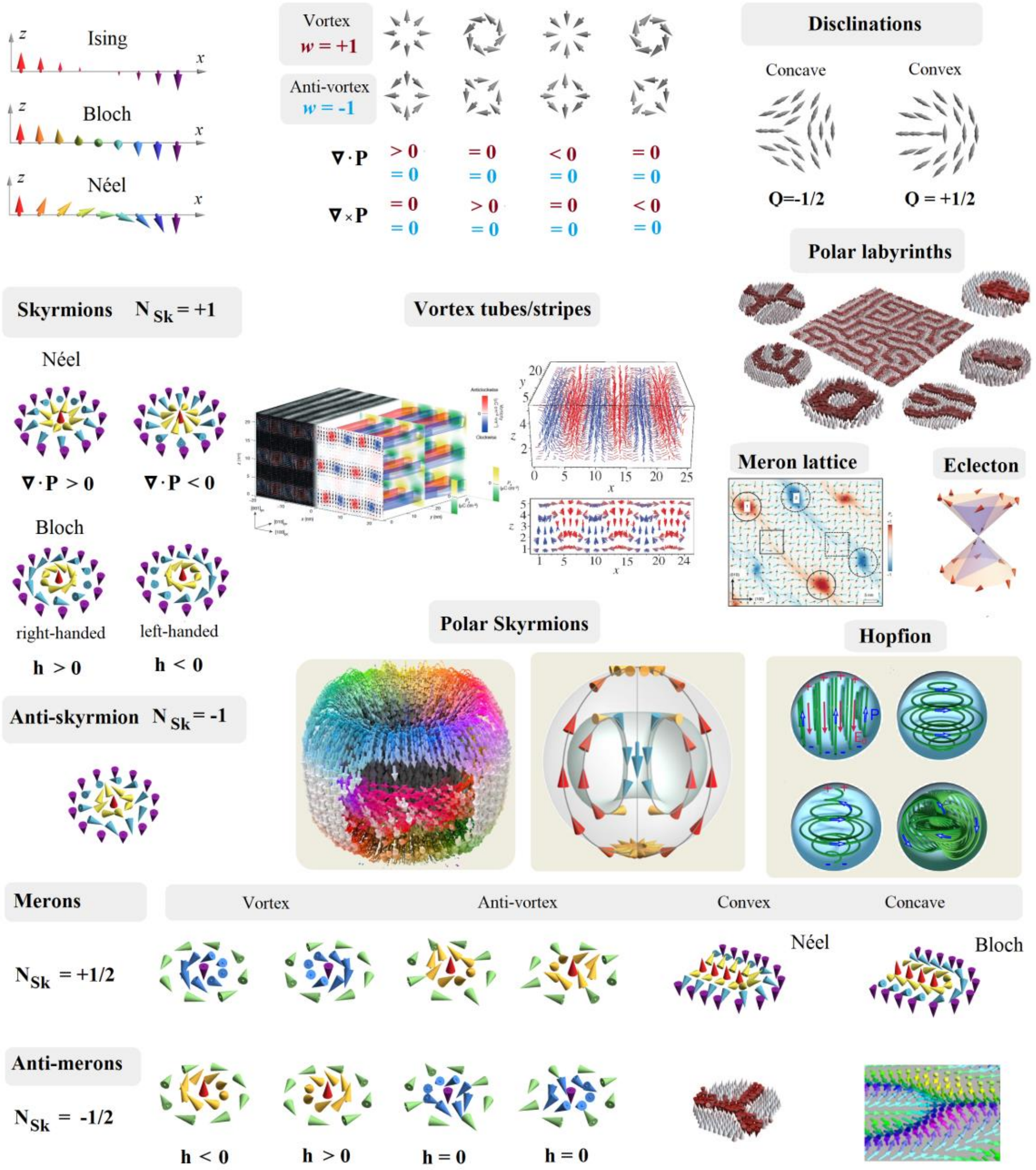

J. Junquera *et al.* Rev. Mod. Phys. **95**, 025001 (2023)

Importance of Mechanical Boundary Conditions

Mechanical boundary conditions can be tuned by changing the substrate on top of which the superlattice is grown

Wide variety of substrates to tune the epitaxial strain $\epsilon = \frac{a_s - a_0}{a_s}$

C. Dai *et al.* Appl. Phys. Lett. **123**, 052903 (2023)

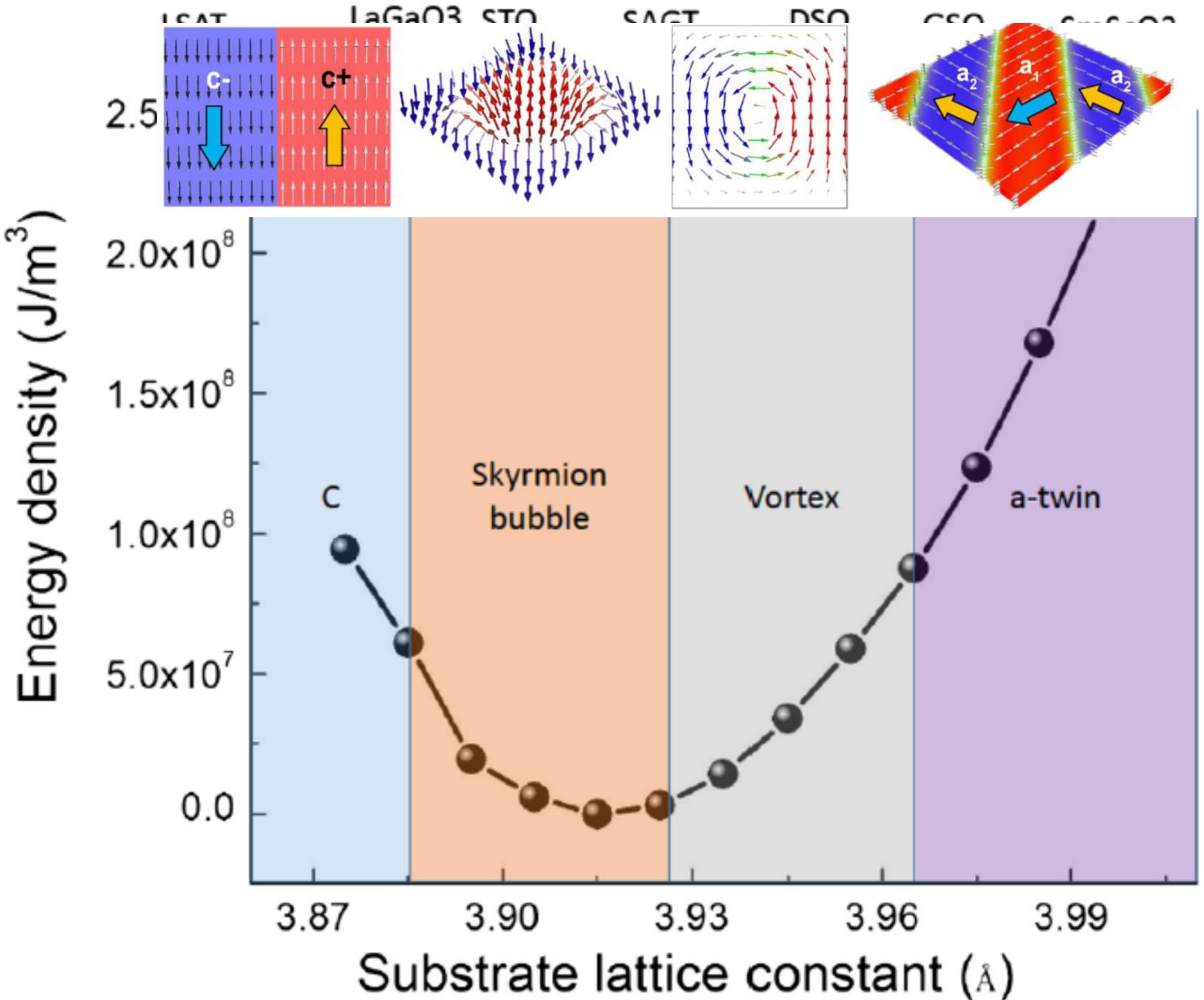

Phase diagram of $(PbTiO_3)_{16}/(SrTiO_3)_{16}$ superlattices as a function of substrate lattice constant

J. Junquera *et al.* Rev. Mod. Phys. **95**, 025001 (2023)

Image courtesy of Z. Hong

Novel topological phases come with exotic functional properties

Negative Capacitance

S. Das,…, F. Gómez Ortiz *et al.* Nat. Mater. **20**, 194 (2021)

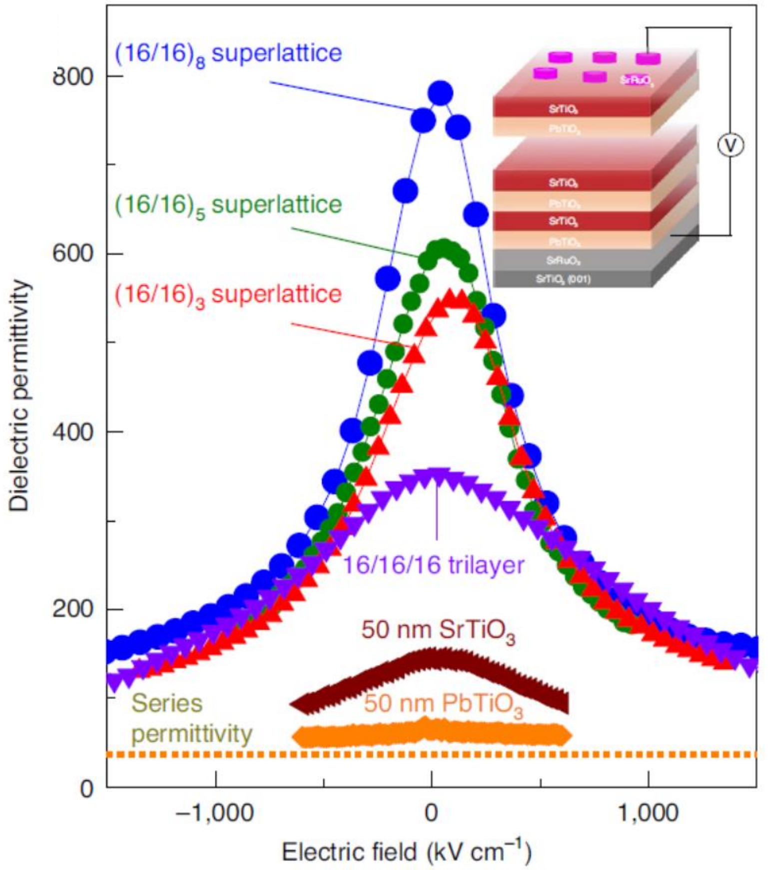

Ultralow-Power computing

Chirality

P. Behera, F. Gómez Ortiz *et al.* Sci. Adv. **8**, eabj8030 (2022)

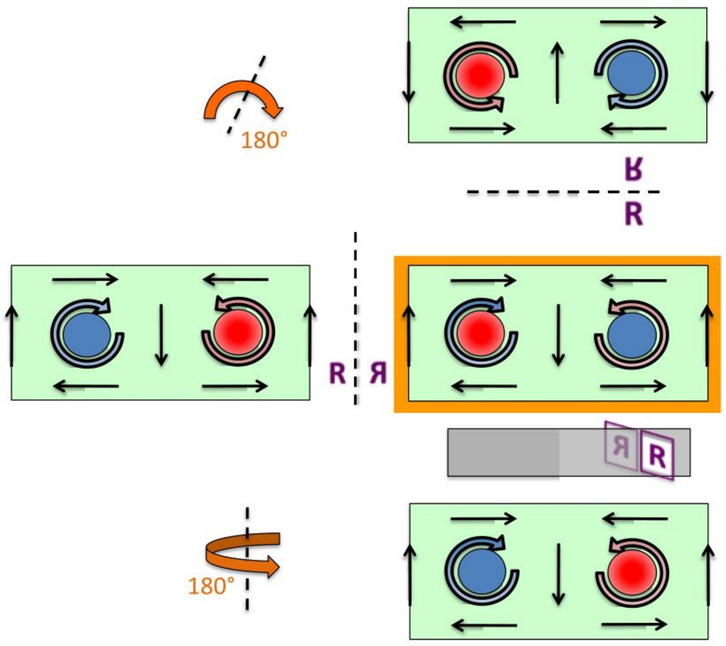

Dynamical properties

P. Behera,…,F. Gómez Ortiz *et al.* Adv. Mater, 2208367 (2023)

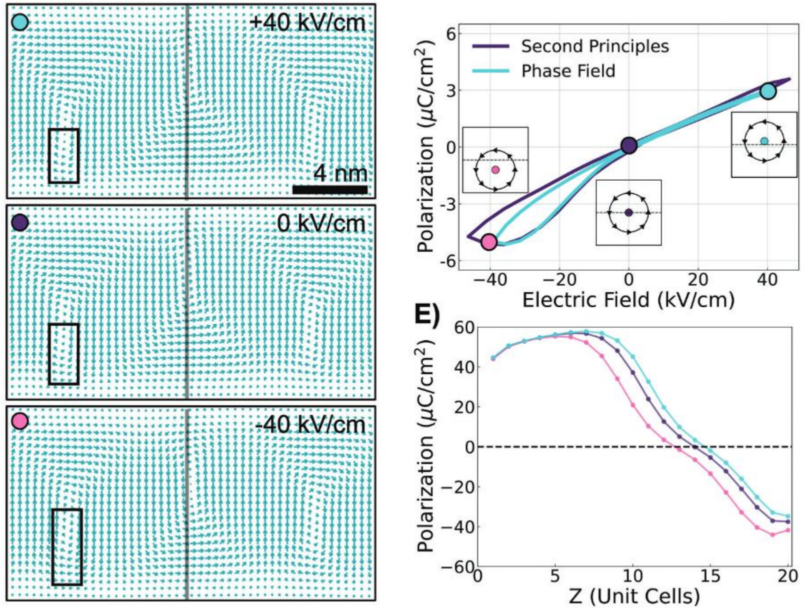

Ultradense memory storage

Chirality emerge at the interface of two achiral materials

L. Louis *et al.* J. Phys.: Condens. Matter **24**, 402201 (2012)

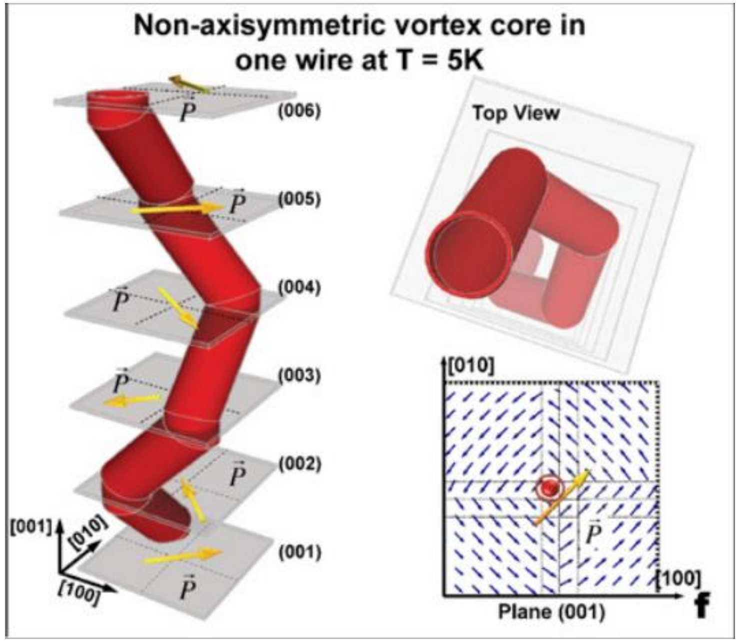

BaTiO$_3$ nanocolumn embedded in SrTiO$_3$ matrix

P.Shafer *et al.* PNAS **115**, 915 (2018)

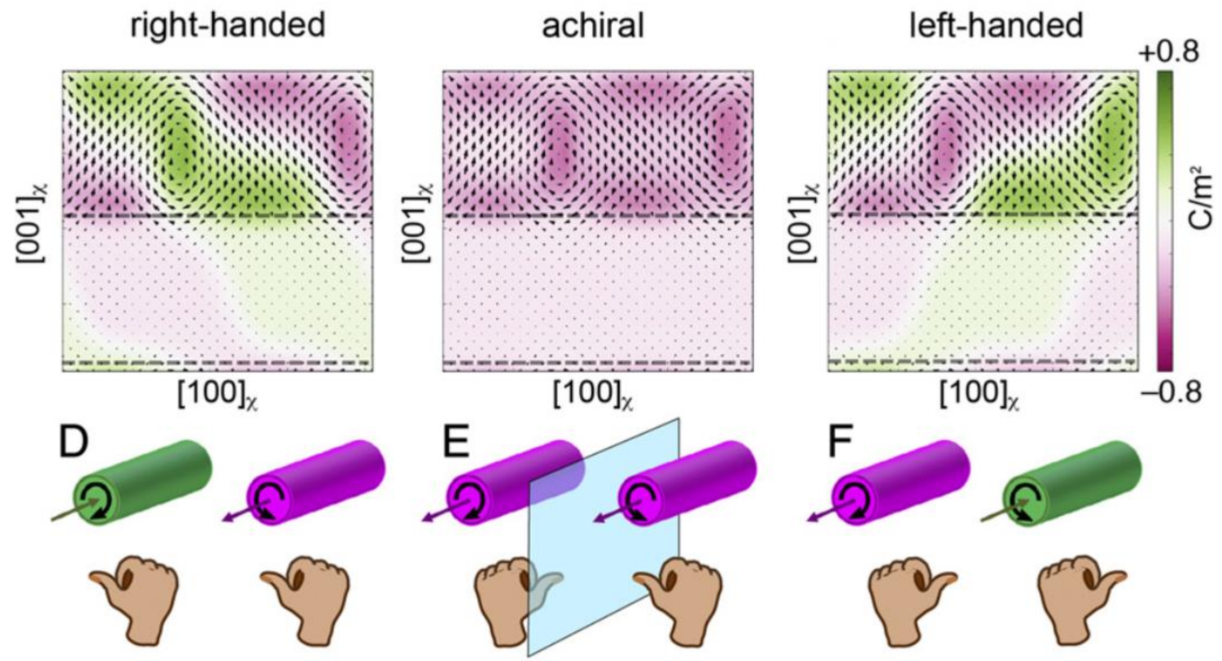

SrTiO$_3$/PbTiO$_3$ superlattices

Goal: generate a chiral structure whose enantiomers can be connected via a controlled transformation

Starting from the achiral structure

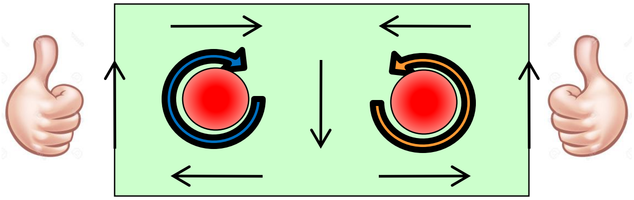

Generate symmetry breakings that can be controlled

Uneven Up/Down domains

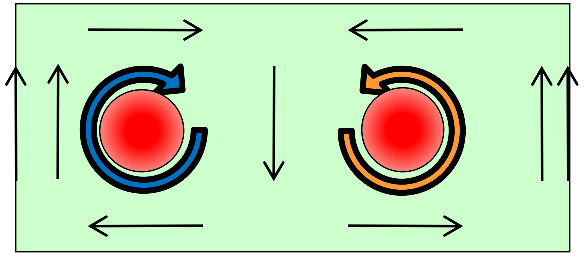

Controllable via $\mathcal{E}_z$

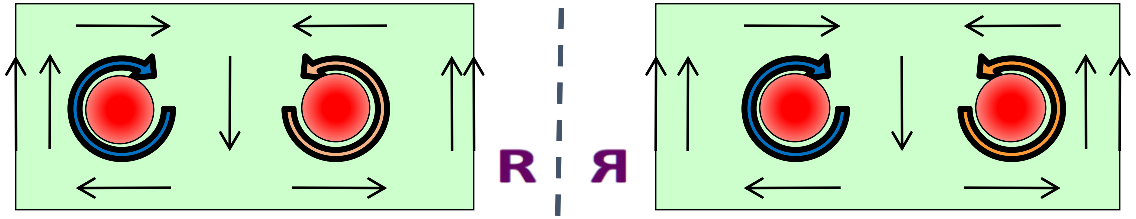

No Chiral

Two different alternatives

Buckling of the vortex cores

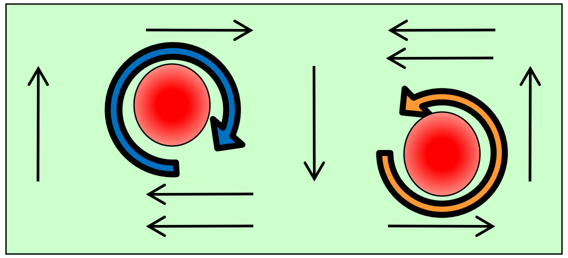

Controllable via $\mathcal{E}_x$

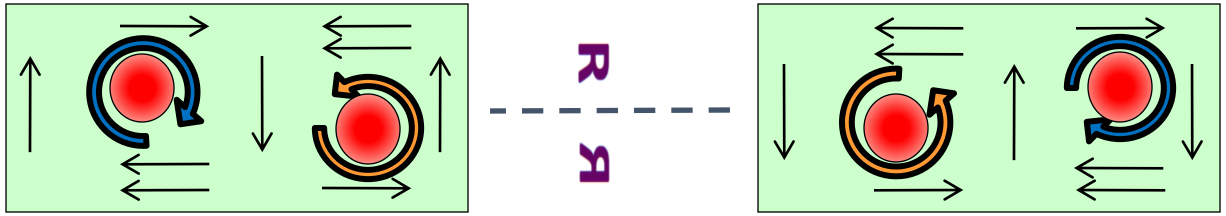

No Chiral

Idea: combine the two previous breaking distortions

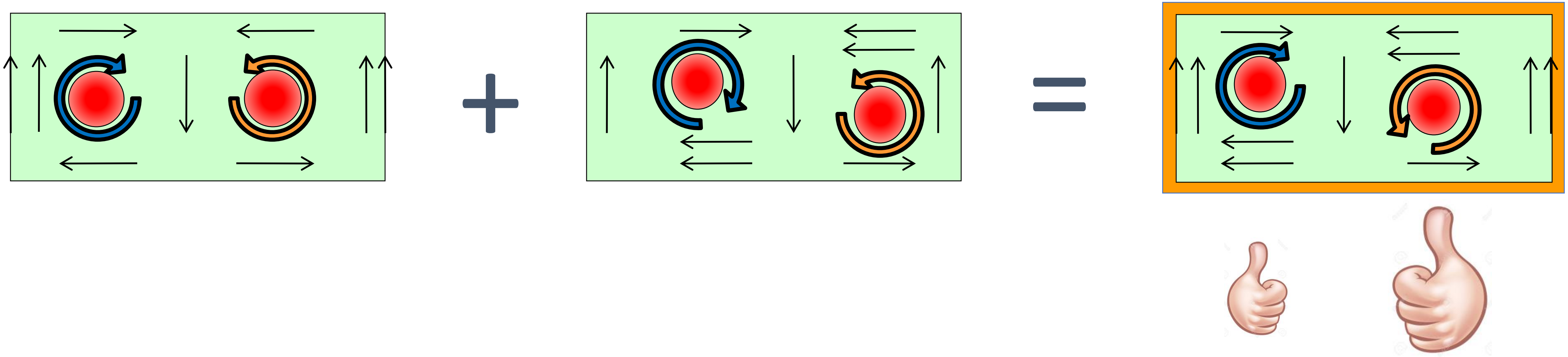

The resulting structure is chiral in 3D

Buckling can be controlled by means of an in plane electric field ($\mathcal{E}_x$)

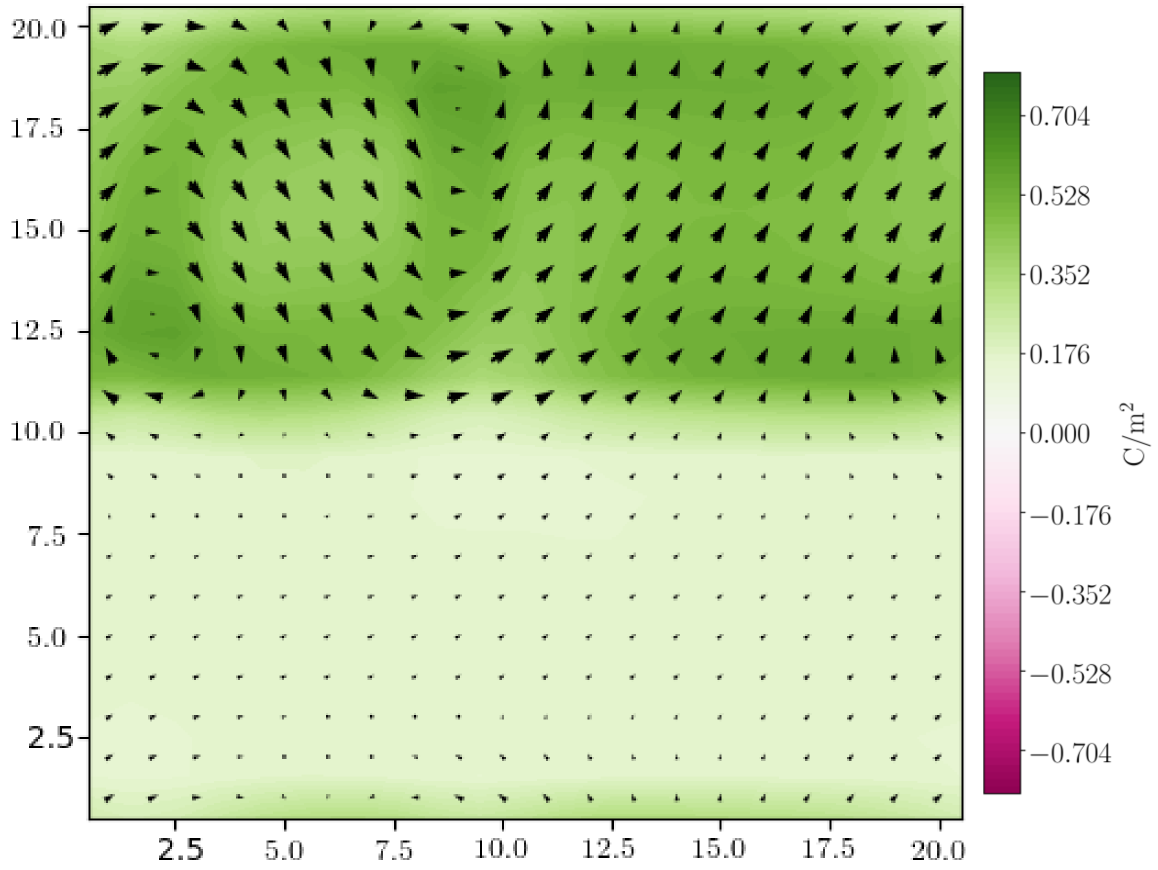

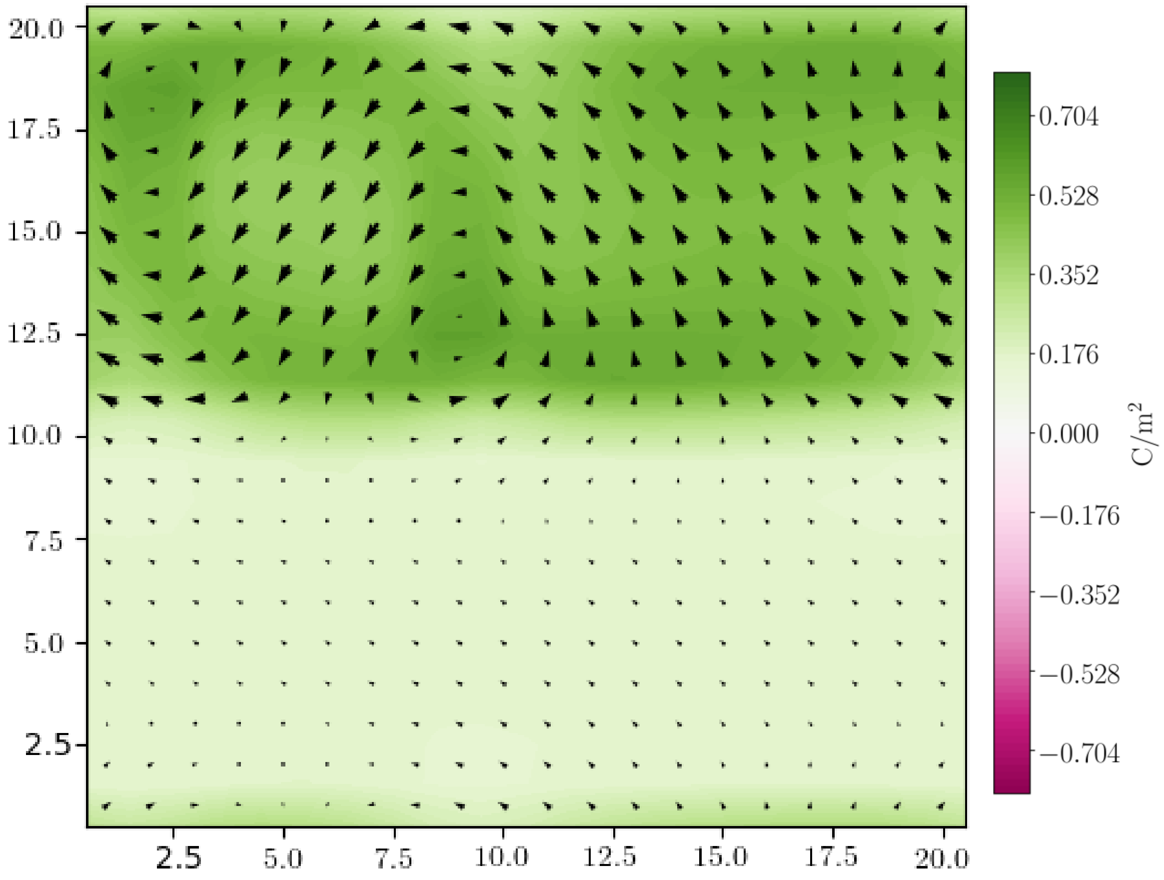

$\mathcal{E}_x > 0 \Rightarrow p_x > 0$ →CW down

$\mathcal{E}_x < 0 \Rightarrow p_x < 0$ →CW up

Electric Field control of Chirality

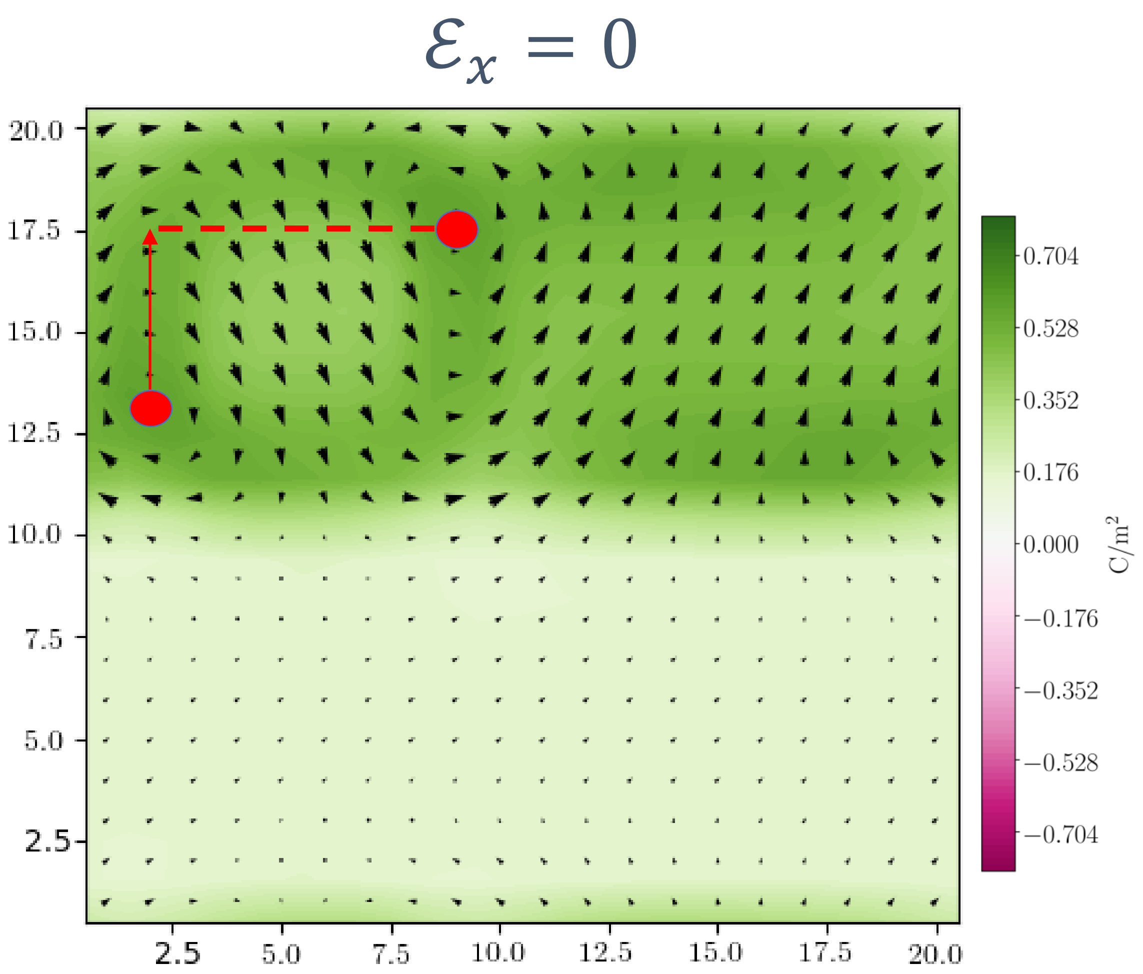

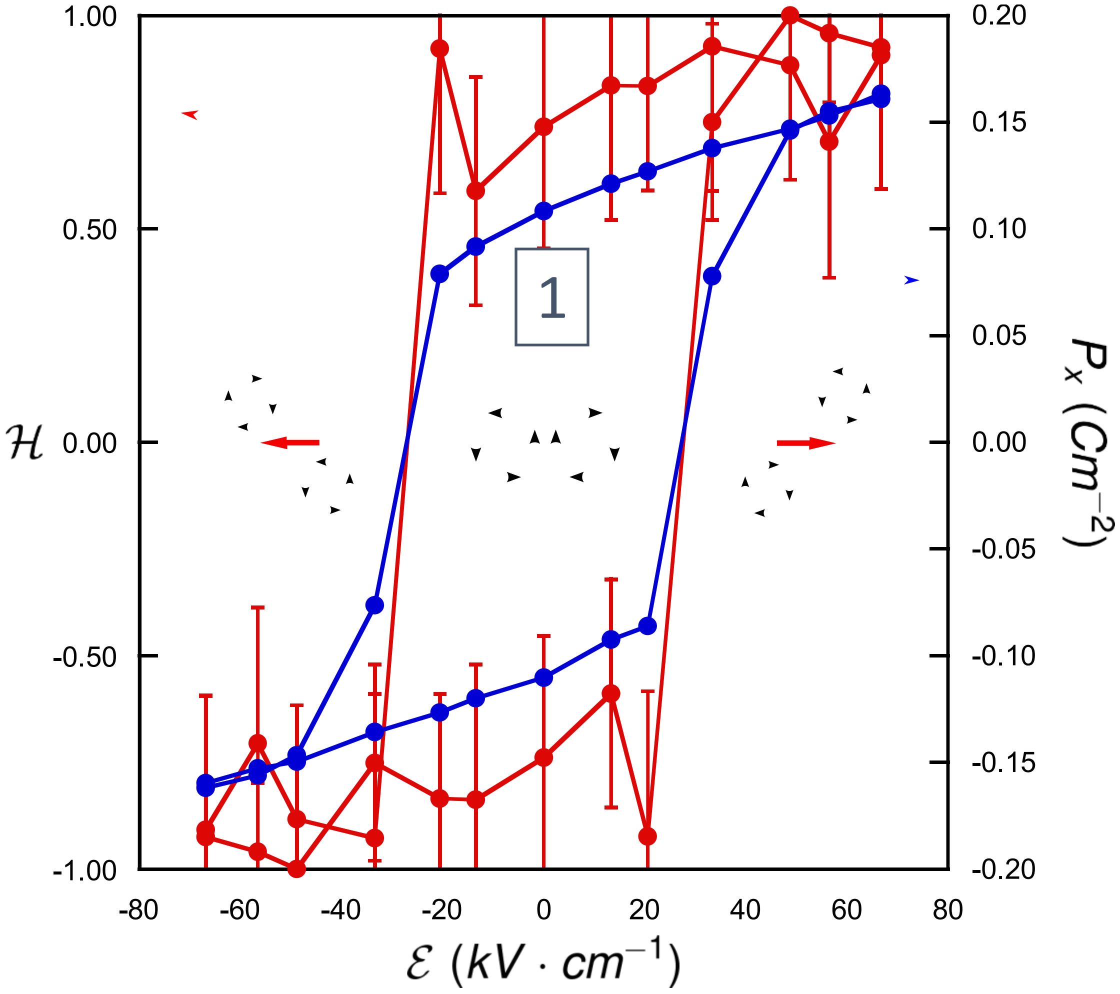

Electric Field control of Chirality

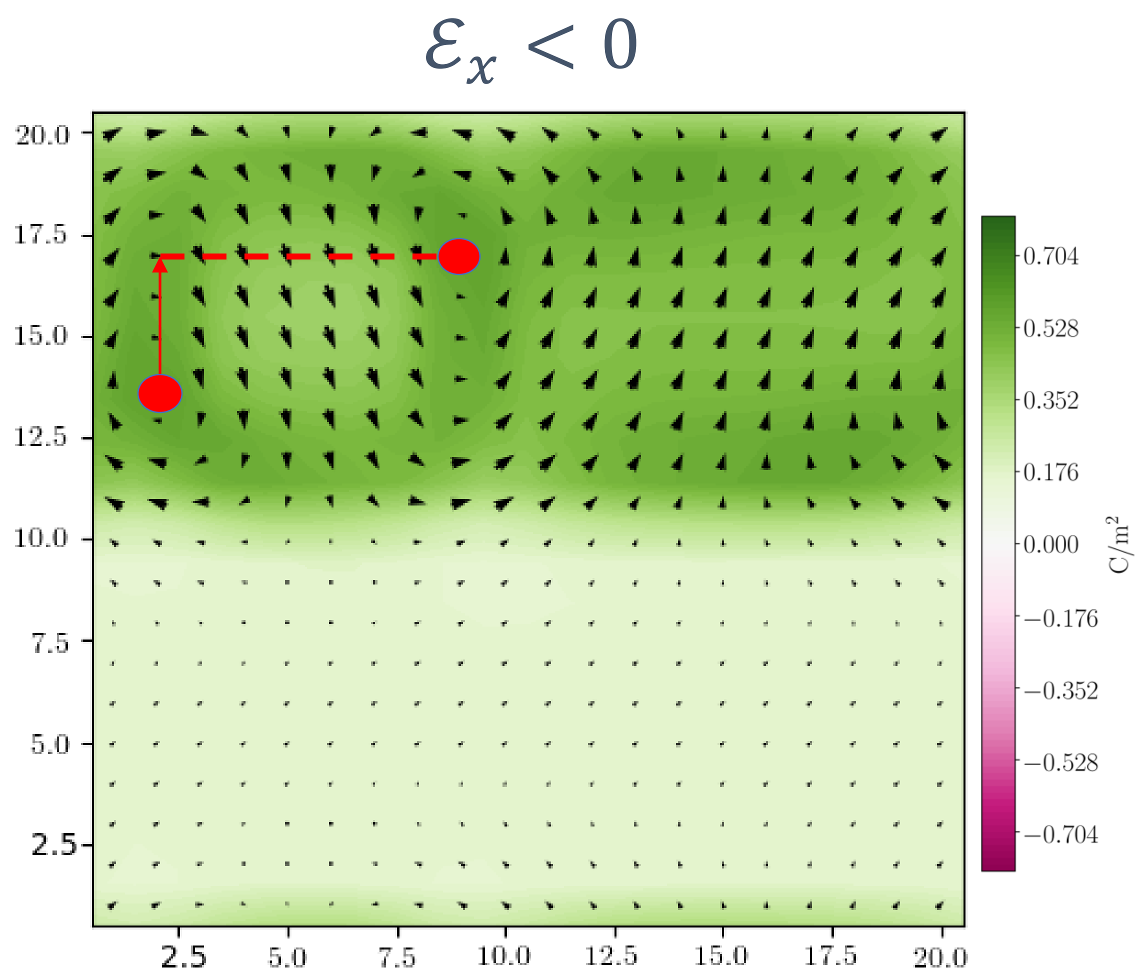

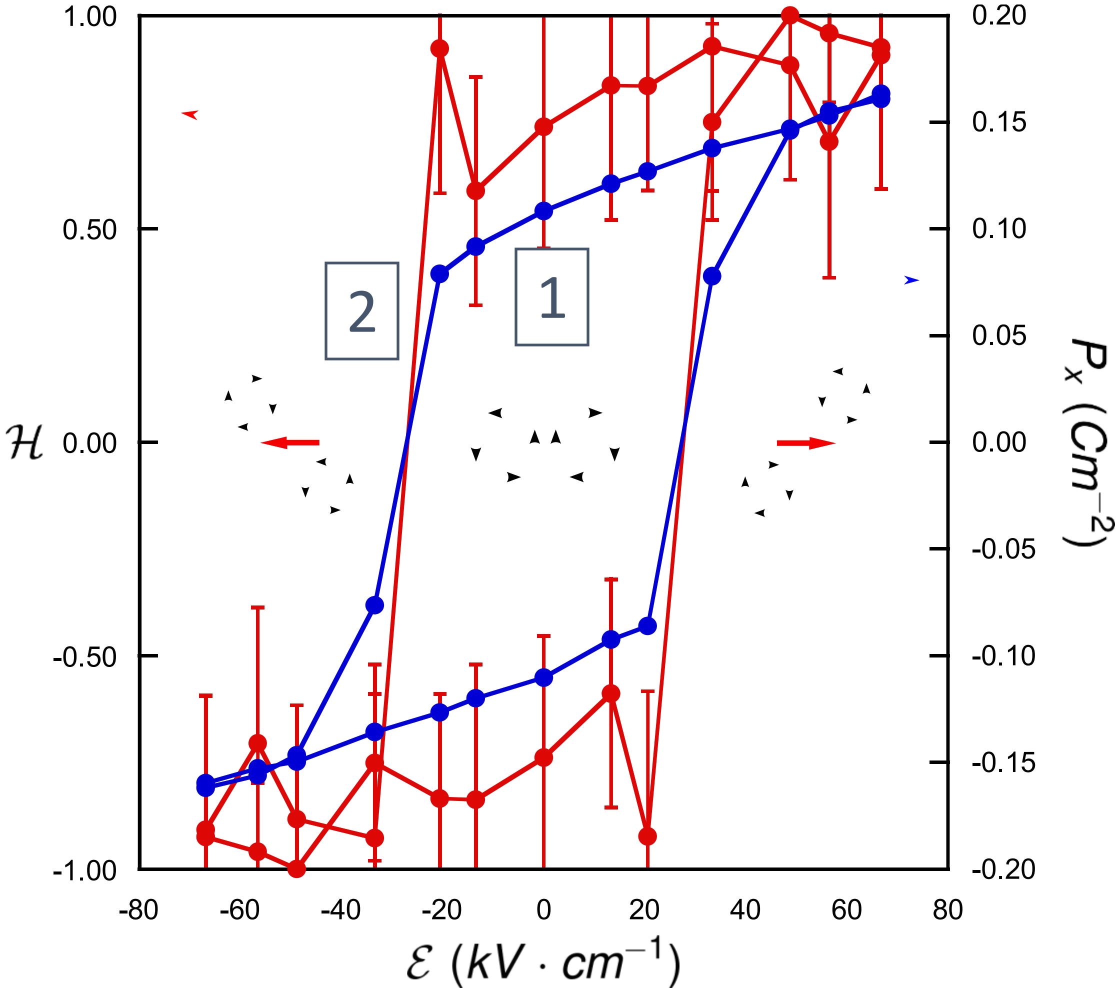

Electric Field control of Chirality

$\mathcal{E}_x < 0$

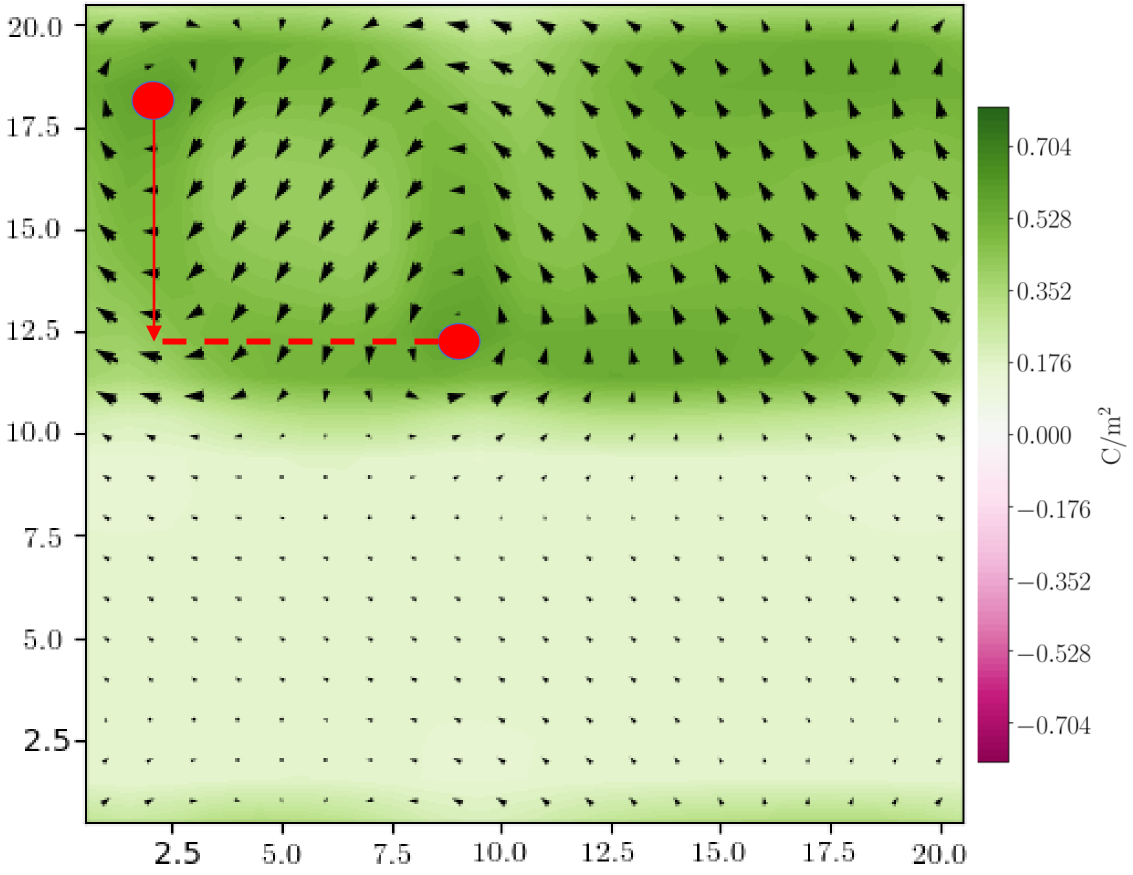

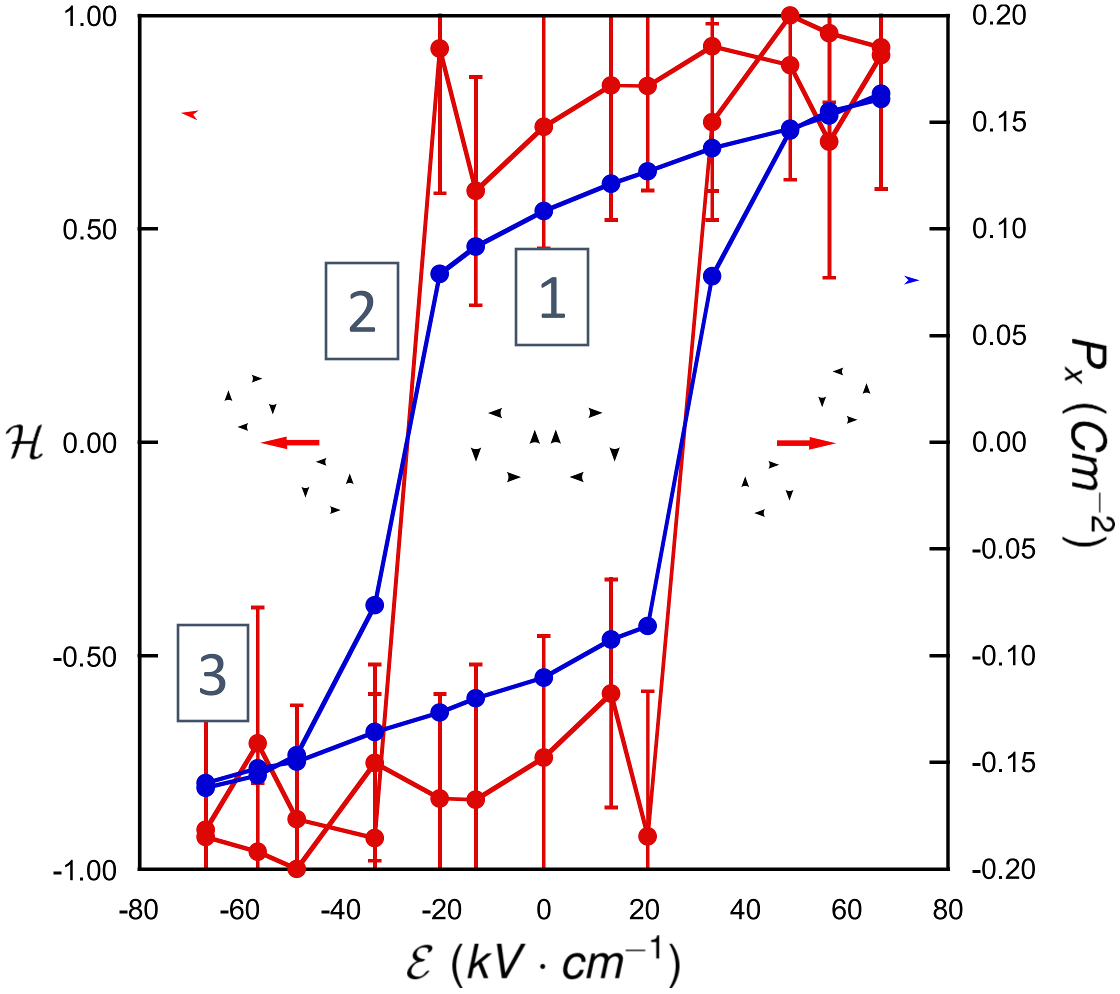

Electric Field control of Chirality

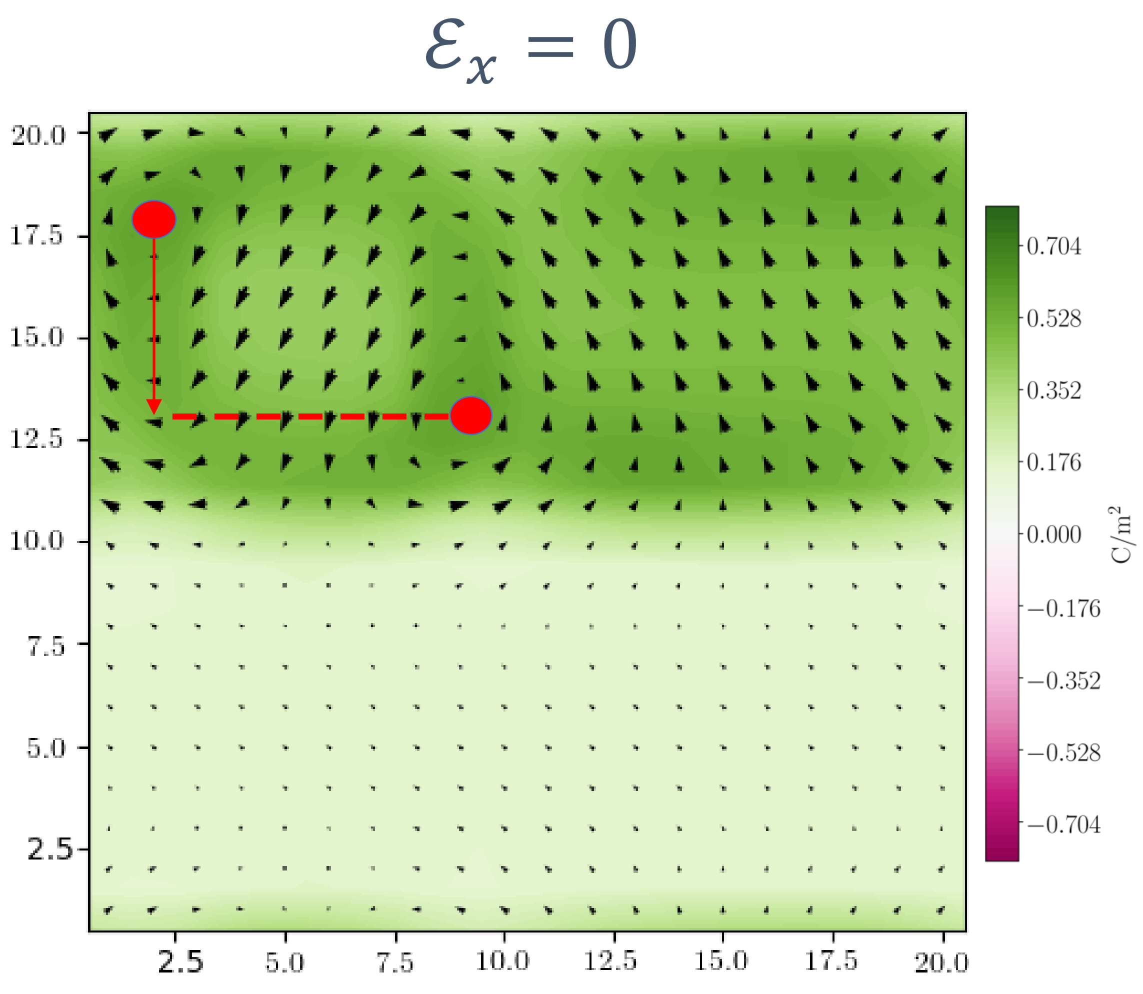

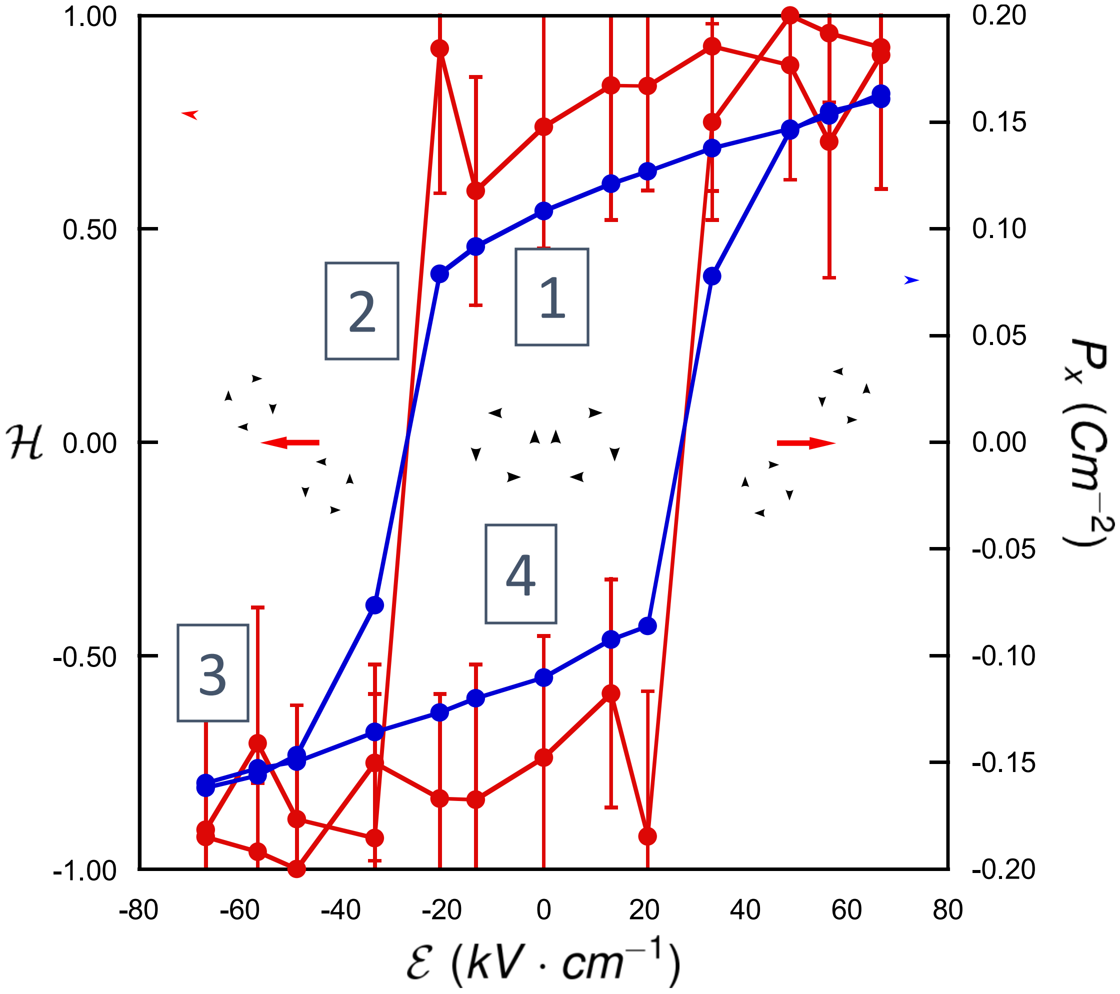

Electric Field control of Chirality

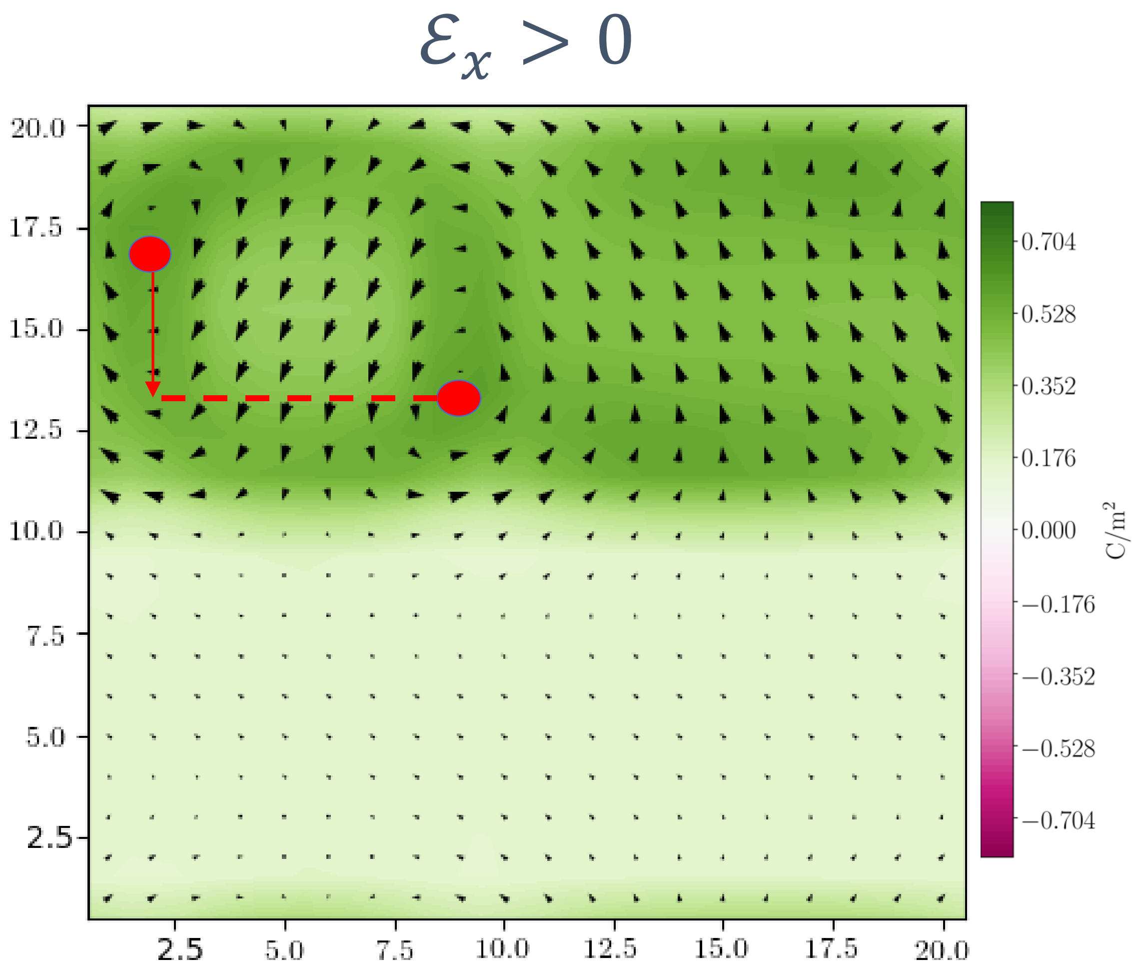

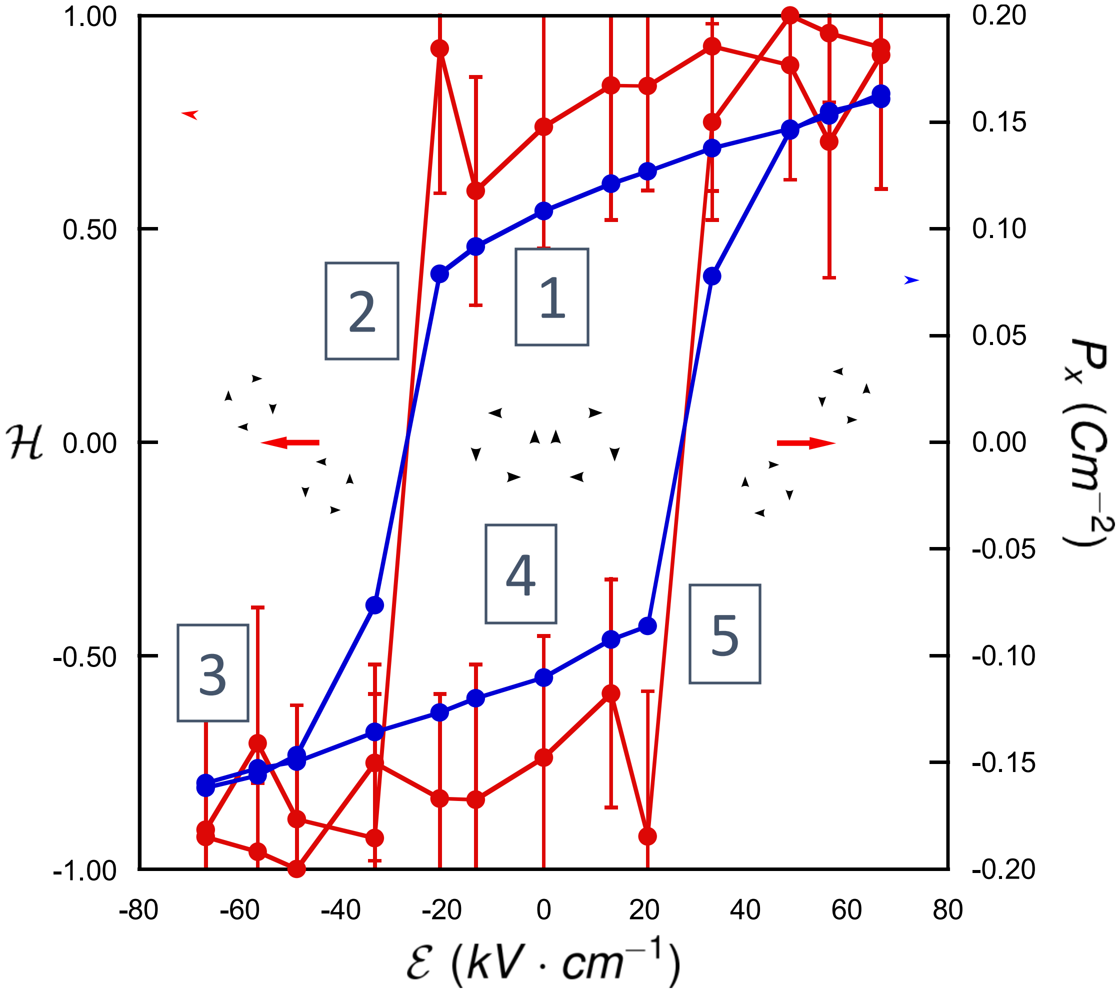

Electric Field control of Chirality

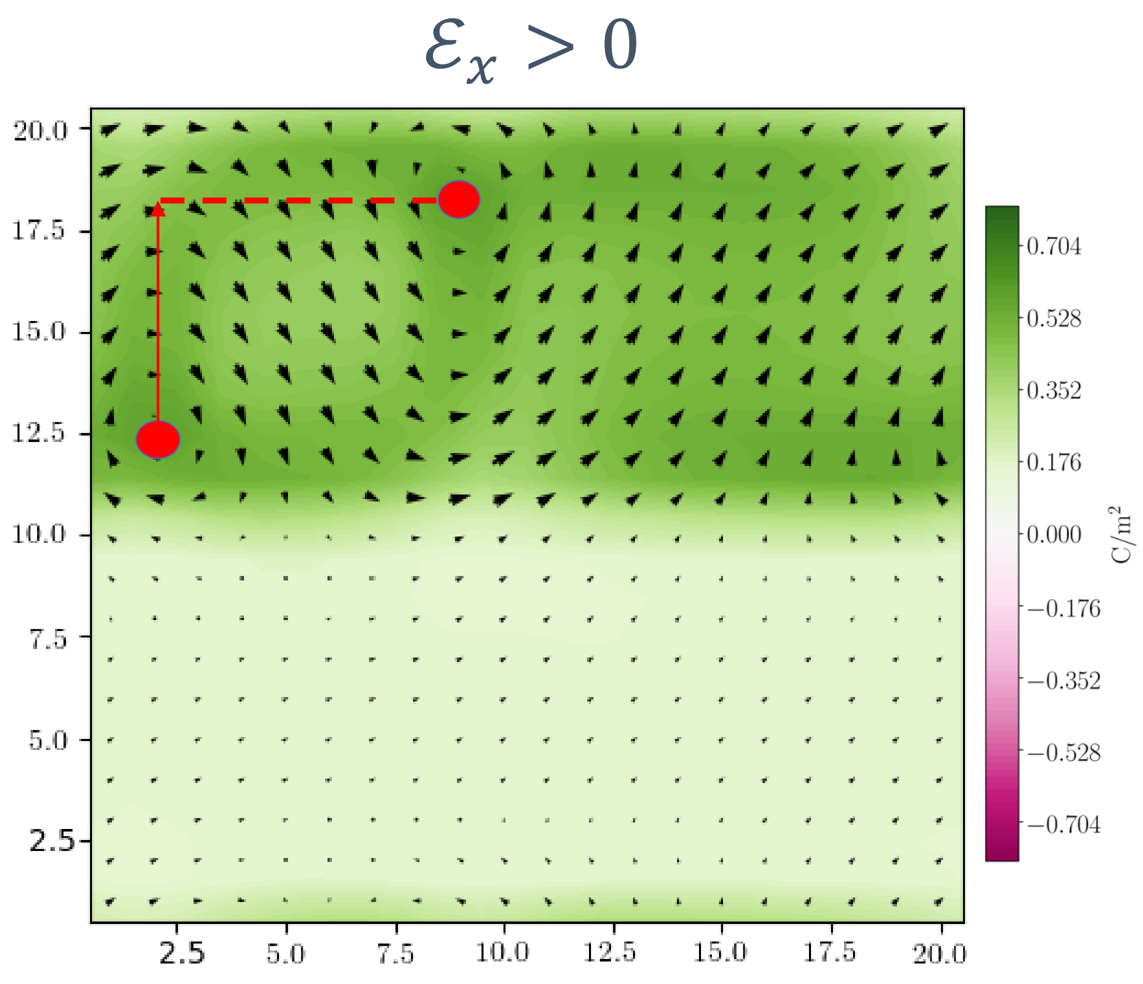

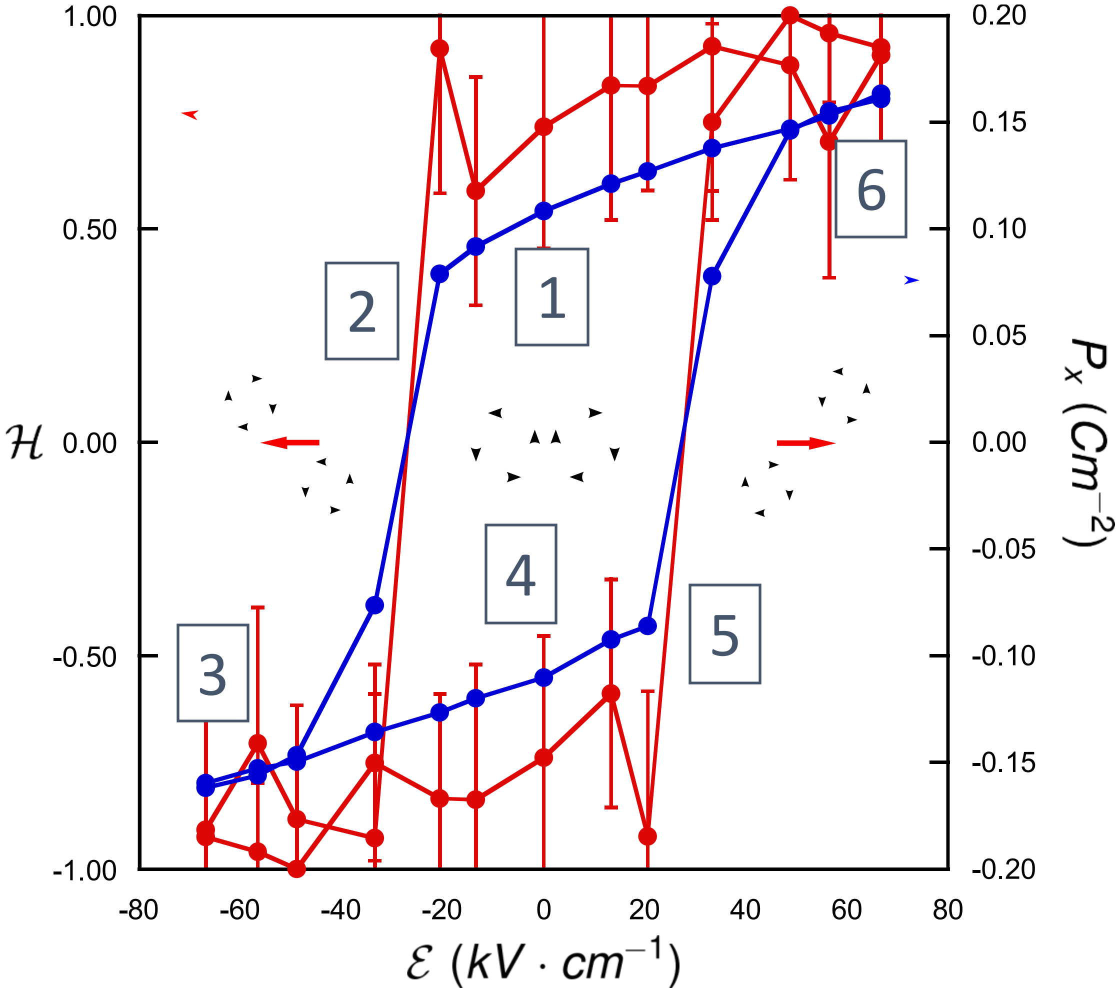

Electric field reversal of chirality confirmed by second-harmonic generation circular dichroism

- Measured H
- Calculated H
- Measured P_x
- Calculated P_x

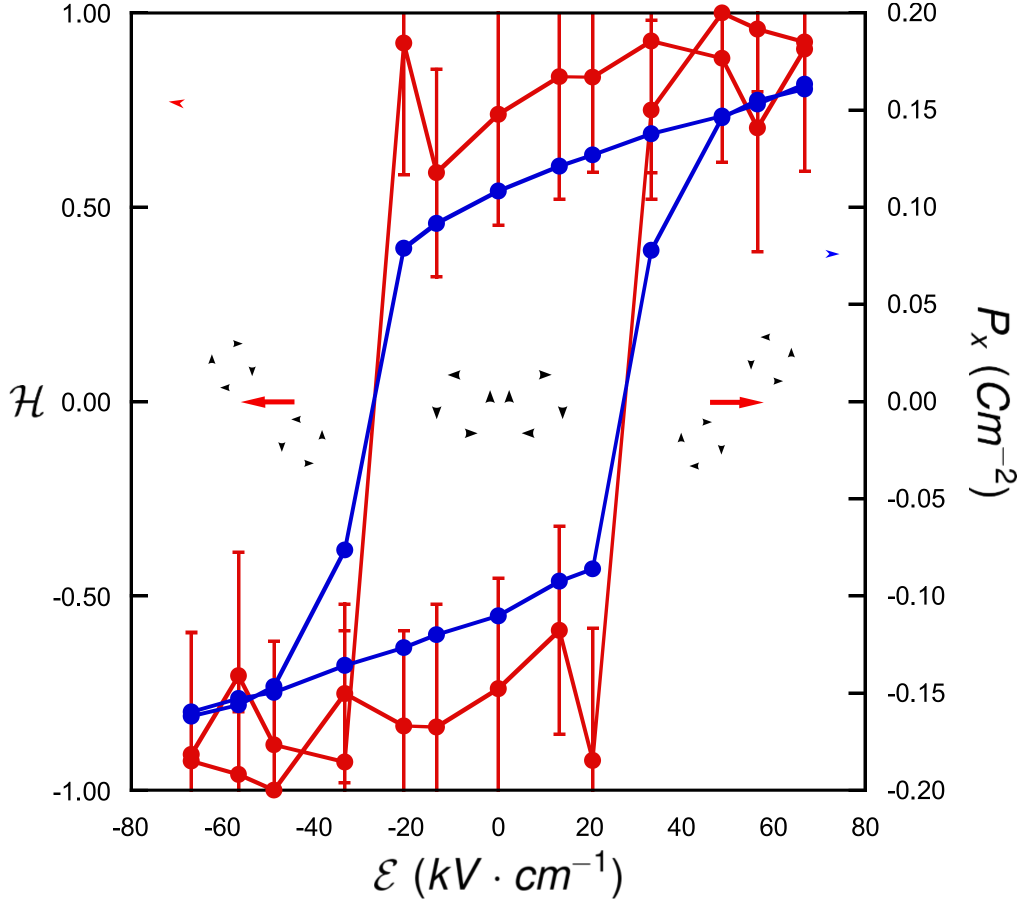

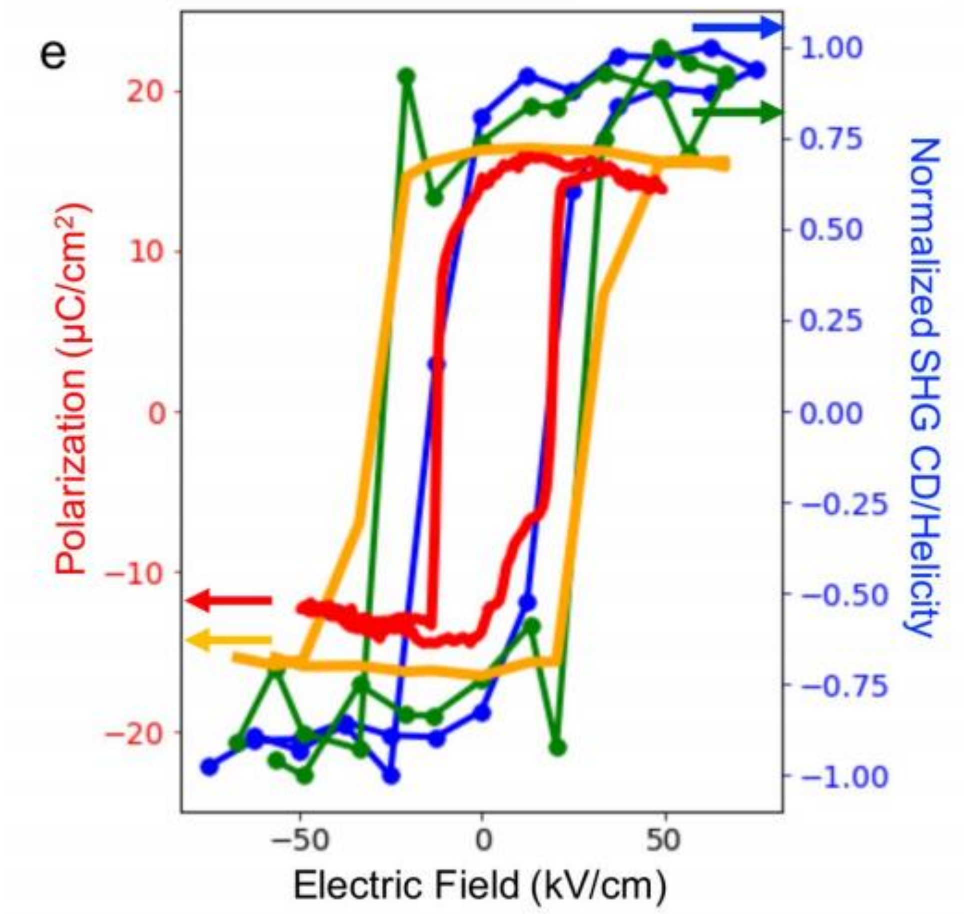

P. Behera, F. Gómez Ortiz *et al*. Sci. Adv. **8**, eabj8030 (2022)

Novel topological phases come with exotic functional properties

Negative Capacitance

S. Das,…, F. Gómez Ortiz *et al.* Nat. Mater. **20**, 194 (2021)

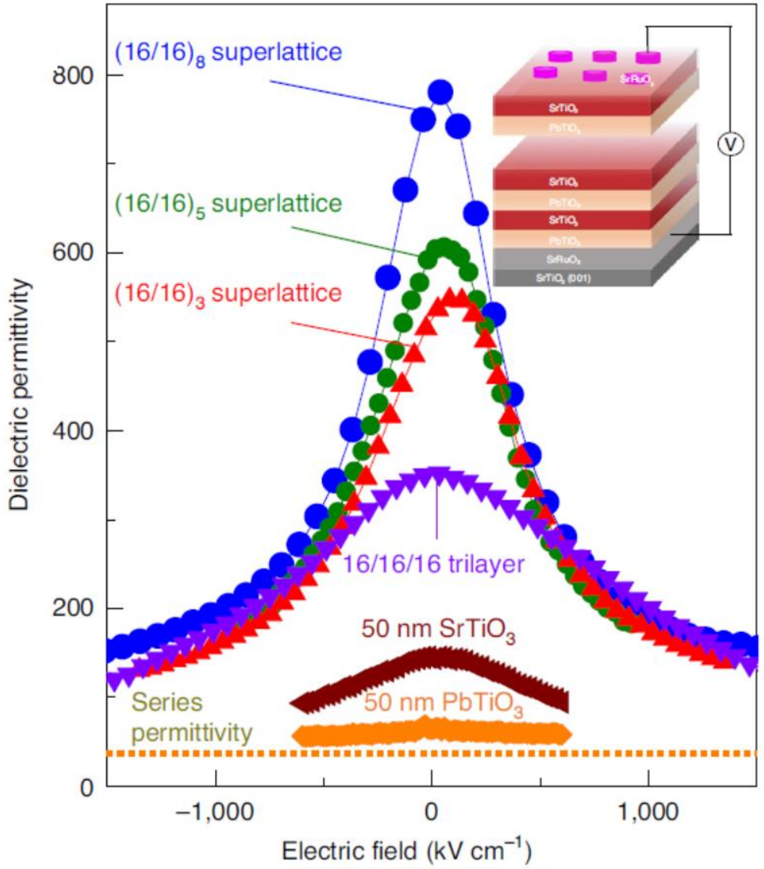

Ultralow-Power computing

Chirality

P. Behera, F. Gómez Ortiz *et al.* Sci. Adv. **8**, eabj8030 (2022)

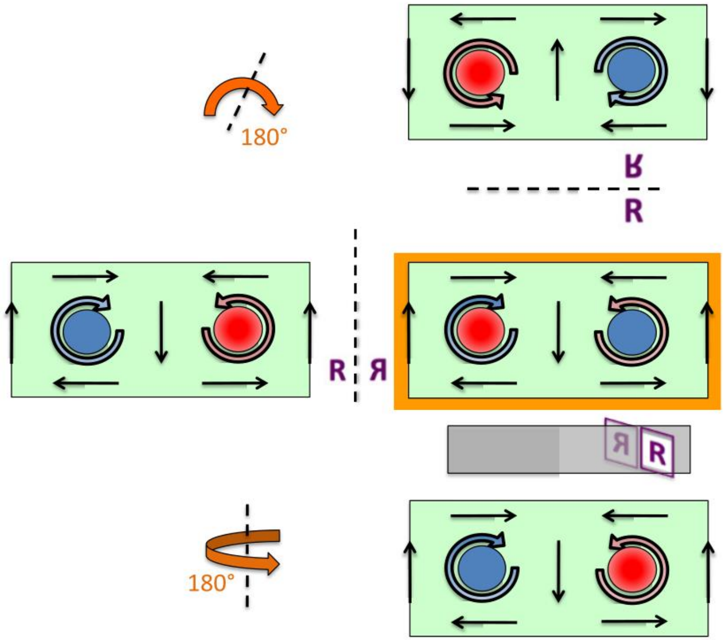

Ultrafast Dynamics

P. Behera,…,F. Gómez Ortiz *et al.* Adv. Mater, 2208367 (2023)

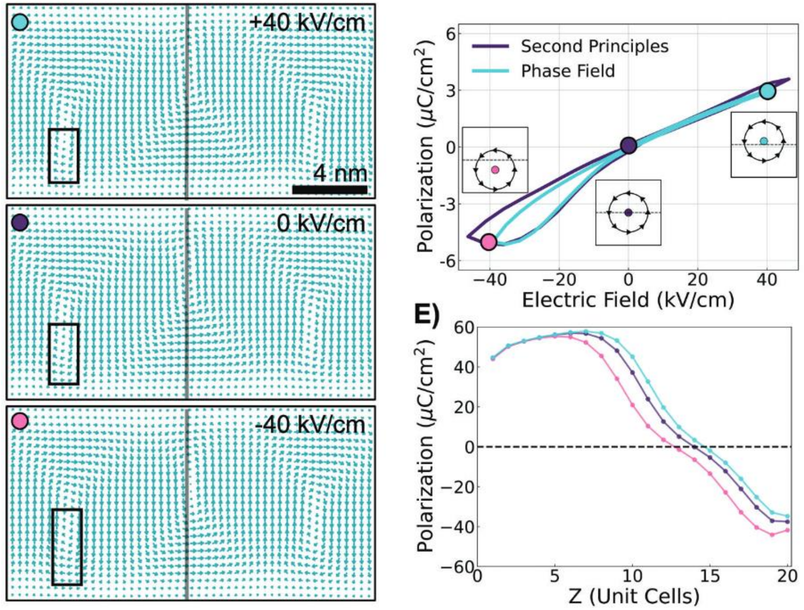

Ultradense memory storage

At high temperatures, $PbTiO_3/SrTiO_3$ superlattices display disordered local dipoles resambling liquid phase

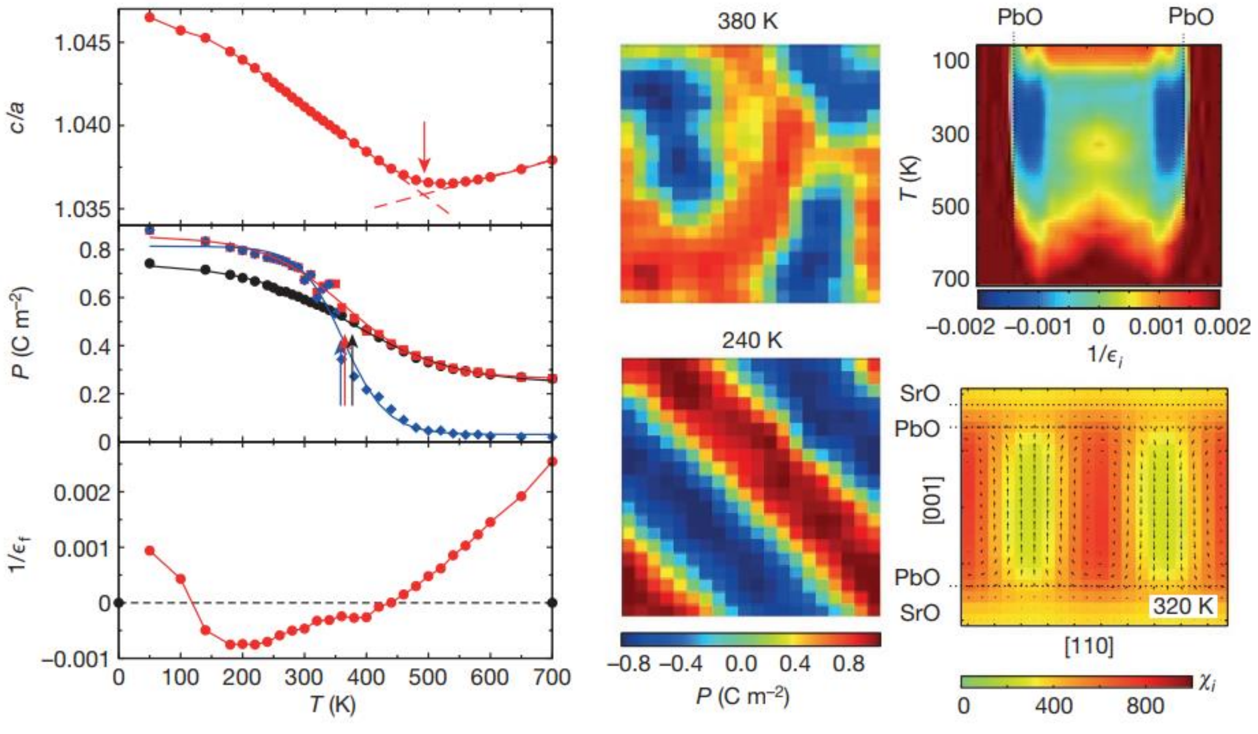

P. Zubko *et al.* Nature **534**, 524 (2016)

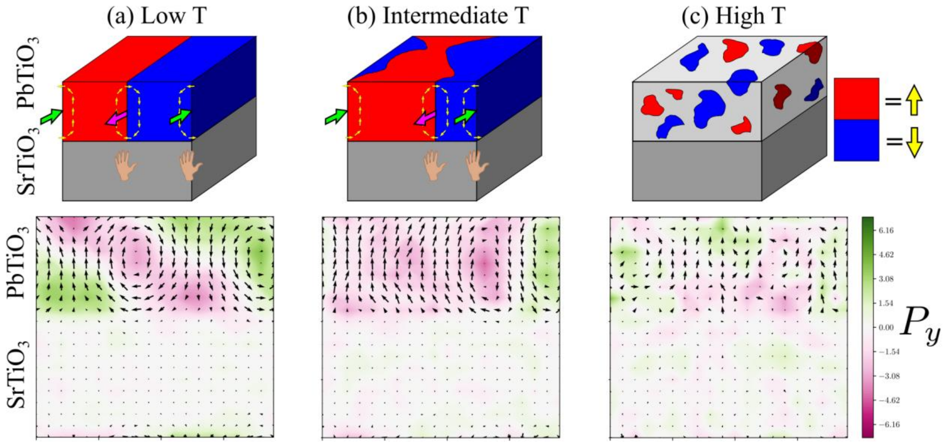

F. Gómez-Ortiz *et al.* Phys. Rev. B **105**, L220103 (2022)

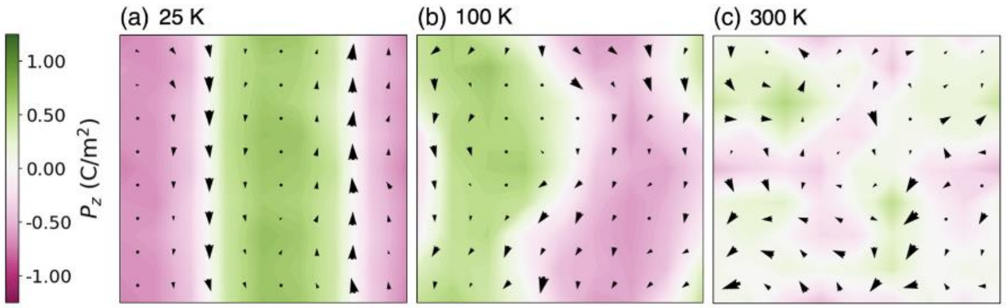

D.E. Murillo-Navarro *et al.* Phys. Status. Solidi RRL **17**, 2300014 (2023)

Mobility of domain walls has been previously predicted and is associated with the onset of the negative capacitance effect

No long-range traslational order of the local dipoles at high temperatures

Low temperature phase (T<270K)
Long range translational and oreintational order

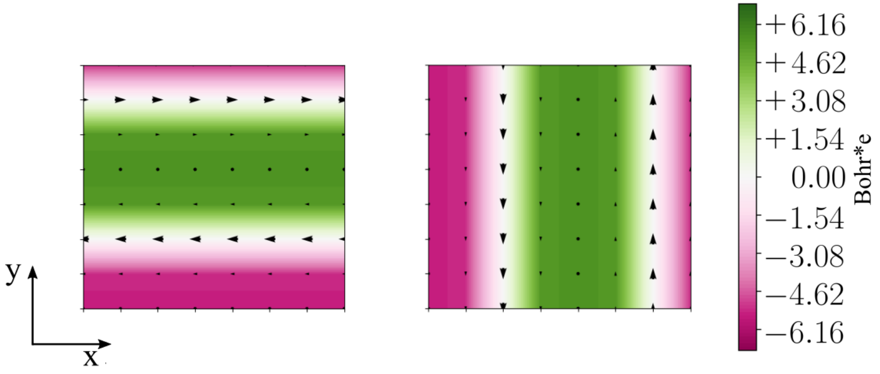

At low temperatures domains arrange along symmetry equivalent directions.

Either x or y oriented domains depending on the realization.

Continuous domain showing translational order along the domain direction

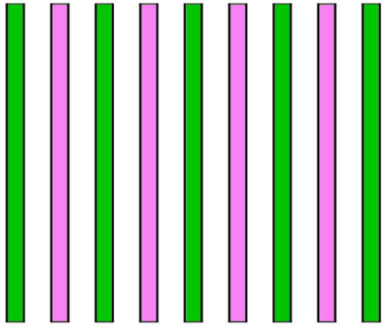

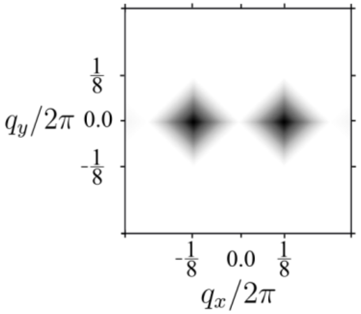

Compute the structure factor of the *z* component of the polarization along the molecular dynamics simulation.

Ordered structure showing a preferred orientation of the domains

$$S(q_x, q_y, t) = \left| \sum_{x=0}^{d-1} \sum_{y=0}^{d-1} e^{-i2\pi(xq_x + yq_y)} \langle P_z(x, y, t) \rangle \right|^2$$

$$S(q_x, q_y) = \langle S(q_x, q_y) \rangle_t$$

Low temperature phase dynamics, T=220K.
Static ordered domains

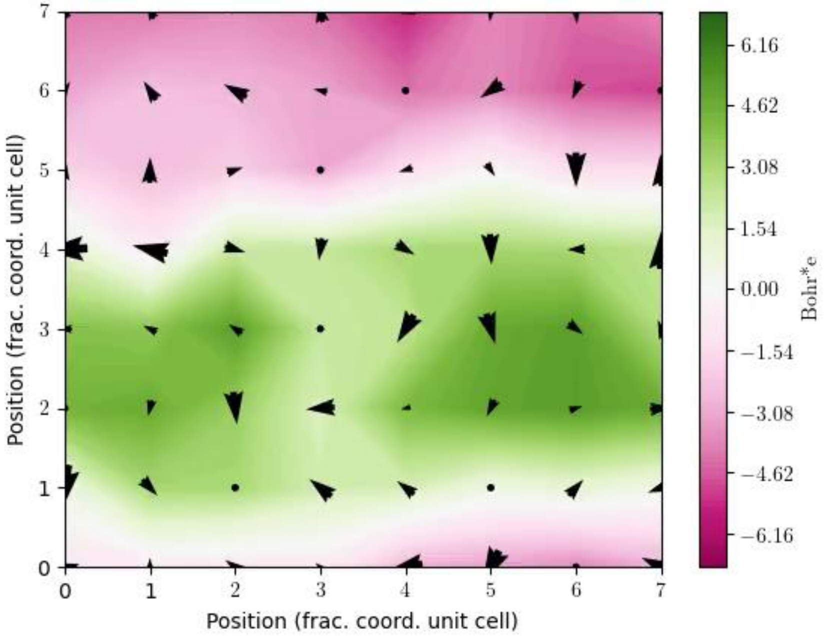

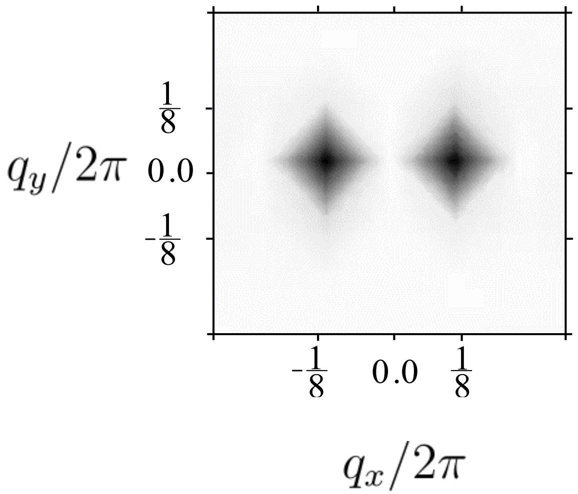

The ferroelectric domains are stable and static

No difference between instantaneous and mean structure factors

Medium temperature phase (280K<T<320K)
Long range oreintational order short range translational order

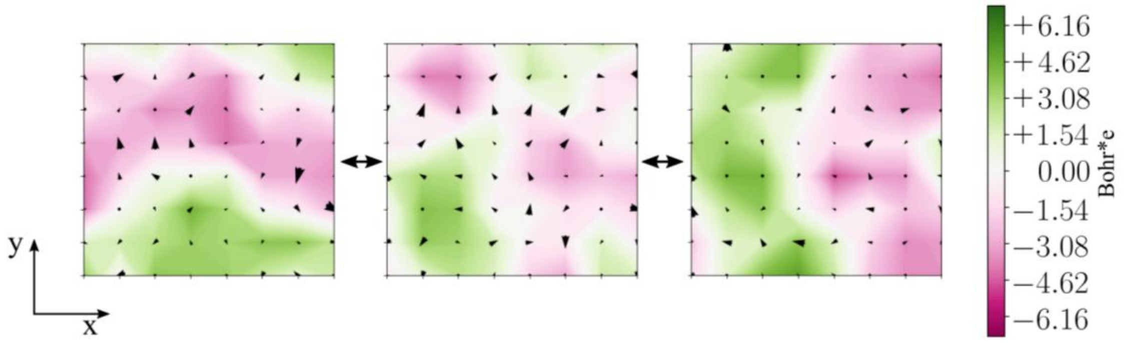

In the intermediate temperature regime domains become mobile.

Meandering domains provoke the los of long-range translational order

Domains transit from *x* to *y* oriented

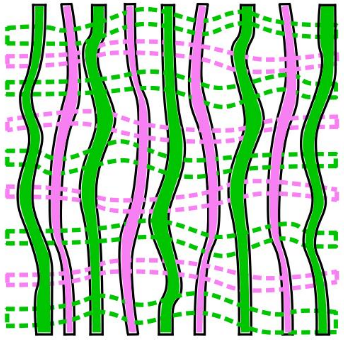

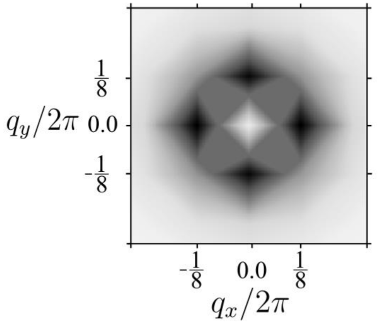

Despite the loss of long-range translational order the system still presents long range orientational order.

Average structure factor shows preferred orientation along *x* and *y*

Medium temperature phase dynamics, T=290K. Fluctuating domains

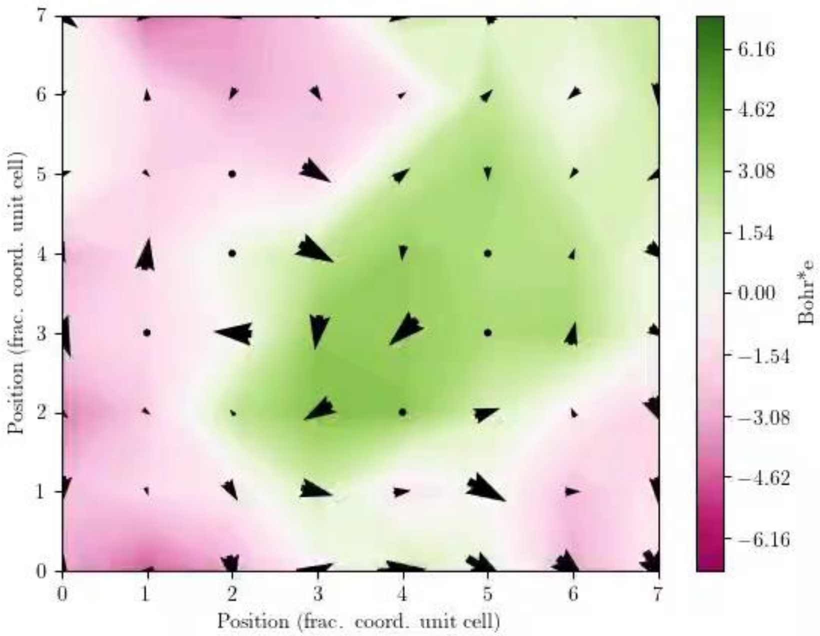

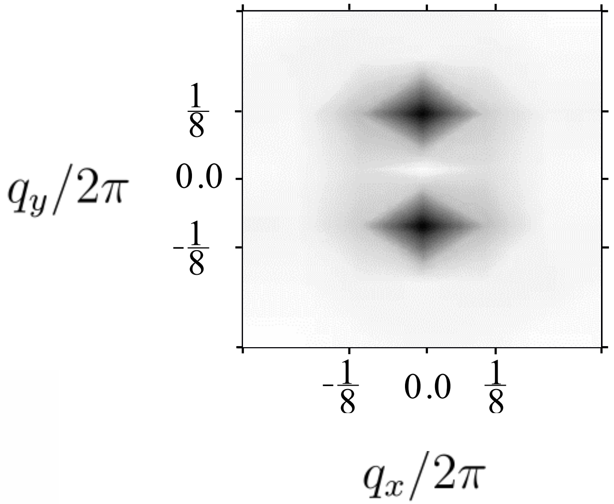

Ferroelectric domains transit back and forth from *x* to *y* oriented

High temperature phase (T>330K)
Short range orientational and translational order

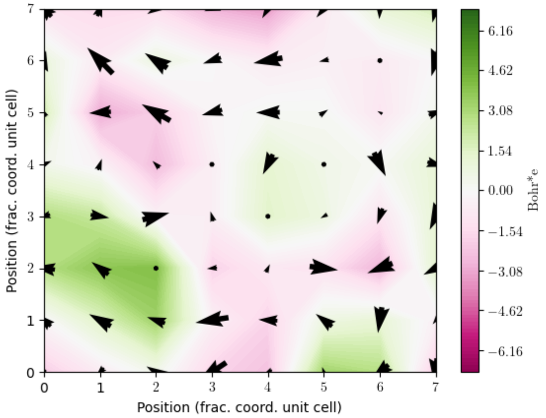

At high temperatures we find a completely disordered phase

Domains arrange in bubles stochastically distributed

Short range translational order as evidenced by the random distribution of the polarization

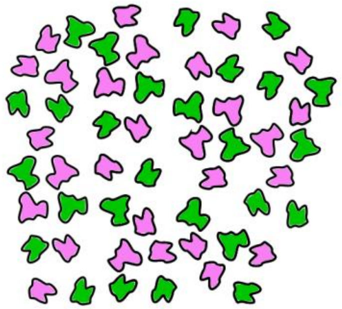

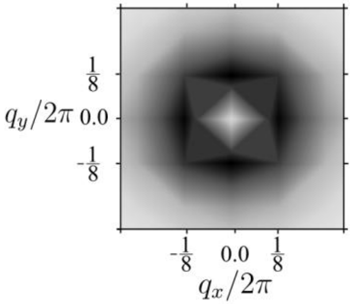

Studying the average structure factor we find that now no preferred direction can be distinguished.

Isotropic distribution along all directions reflecting the short-range orientational order.

High temperature phase dynamics, T=350K. Disordered isotropic state

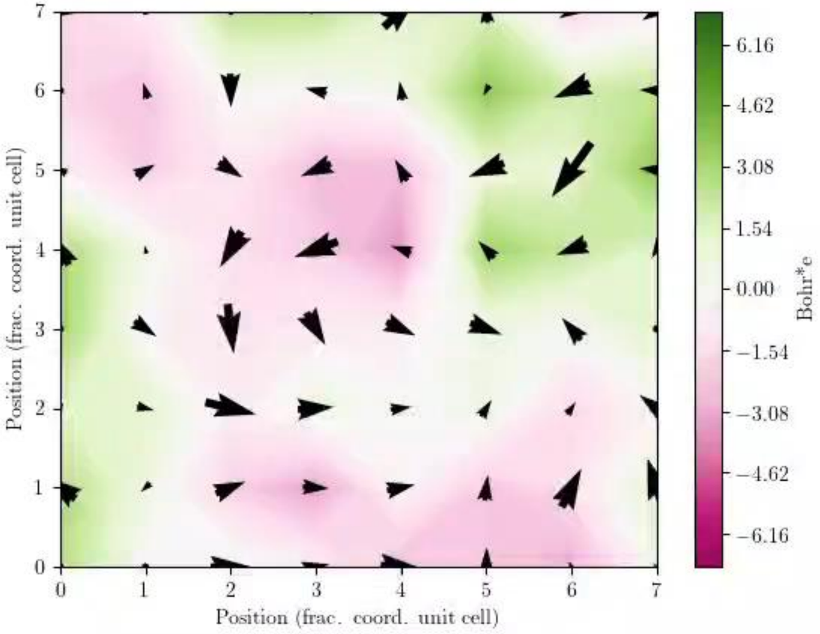

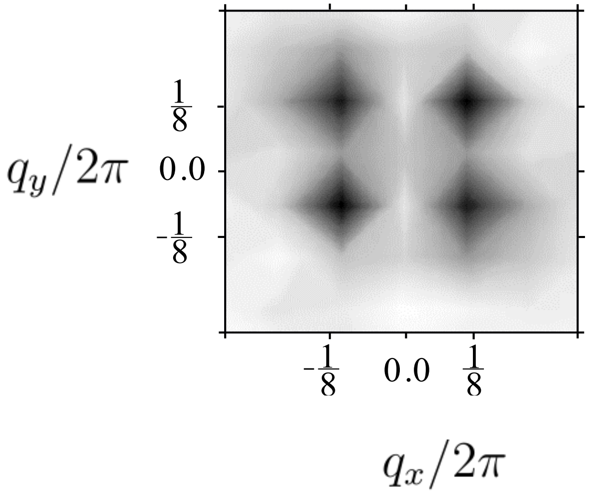

Stochastic motion of the domains.

Hoping rate between *x* and *y* oriented domains as a function of temperature studying structure factors

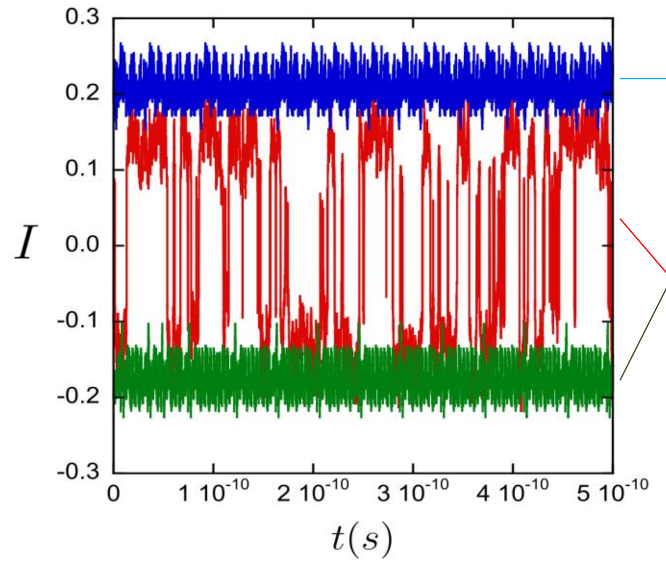

Low temperature static domains in different realizations

Intermediate temperature (T=280K) fluctuating domains

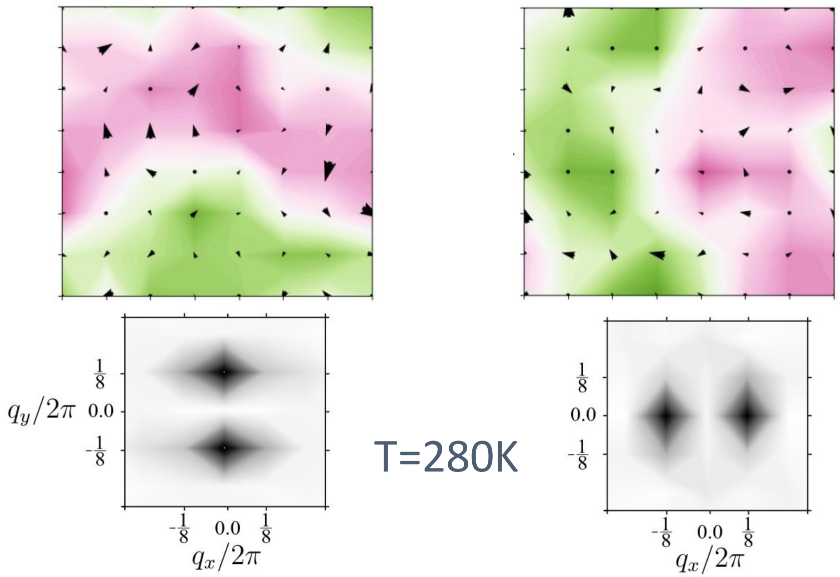

$$I = \begin{cases} \dfrac{|S(\pm\frac{2\pi}{d},0)|^2}{\sum_{q_x,q_y} |S(q_x,q_y)|^2} & \text{if} S(\pm\frac{2\pi}{d},0) > S(0,\pm\frac{2\pi}{d}), \\ -\dfrac{|S(0,\pm\frac{2\pi}{d})|^2}{\sum_{q_x,q_y} |S(q_x,q_y)|^2} & \text{if} S(\pm\frac{2\pi}{d},0) < S(0,\pm\frac{2\pi}{d}). \end{cases}$$

Studying instantaneous structure factors we can determine if the system is preferently *x* or *y* oriented.

X oriented domain ($I < 0$).
Y oriented domain ($I > 0$)

As a function of temperature the number of hopings will vary

F. Gómez-Ortiz et al. arXiv:2401.13026 Accepted in Phys. Rev. Lett.

Thermally activated process following Vogel-Flucher relation

Temperature dependent frequencies ranging from tens of gigahertz to terahertz

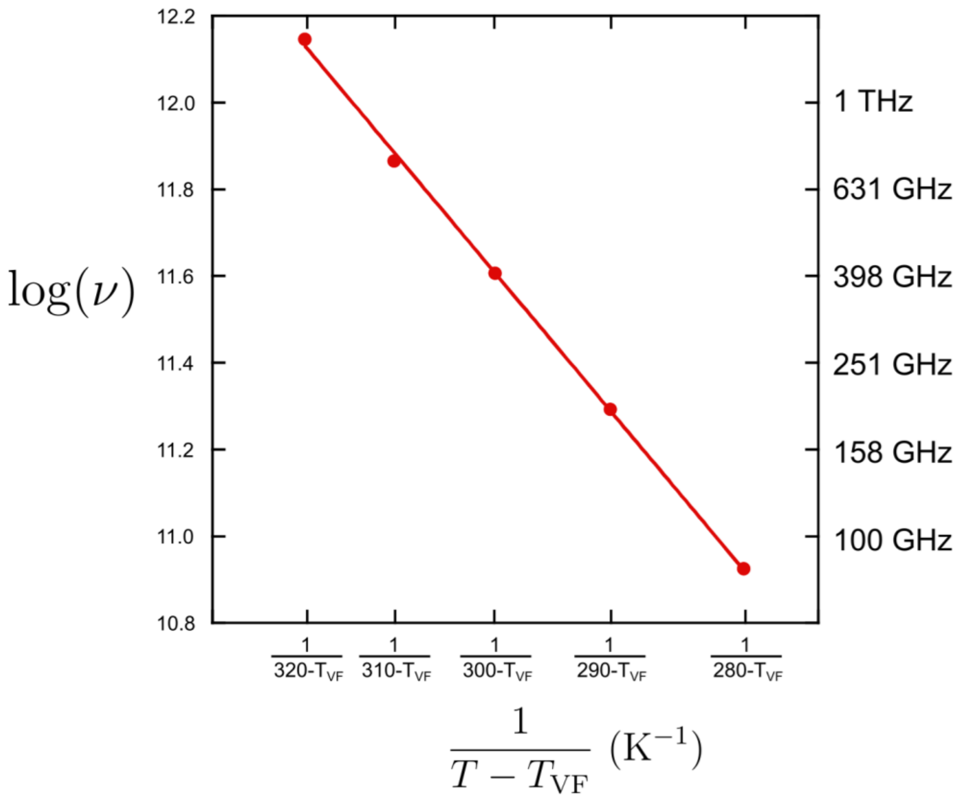

$$\log(\nu) = a + \frac{-E_{\mathrm{VF}}}{k_{\mathrm{B}}(T - T_{\mathrm{VF}})}$$

Domain fluctuation is a cooperative behaviour modeled by Vogel-Flucher relation

$$a = 16.06 \pm 0.07$$
$$E_{\mathrm{VF}} = 57.8 \pm 0.9 \text{ meV}$$
$$T_{\mathrm{VF}} = 150 \pm 40 \text{ K}$$

In principle we should expect to observe domain fluctuation at T_{VF}.

However, at a very low frequency rate. Our simulations are not so large. We are limited to $10^{-9}\mathrm{s}$ and therefore unable to detect events with frequencies lower than $10^{9}\mathrm{Hz} \rightarrow 240 \pm 40\mathrm{K}$.

F. Gómez-Ortiz et al. arXiv:2401.13026 Accepted in Phys. Rev. Lett.

Conclusions

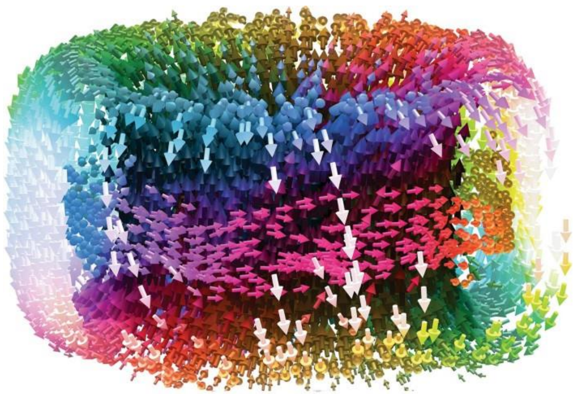

Multitude of fascinating polar textures emerge in ferroelectric materials

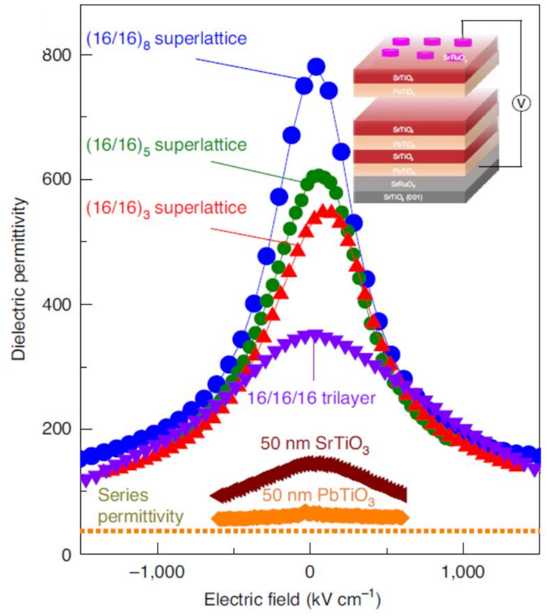

Particle like behaviour and multitude of fascinating functional properties

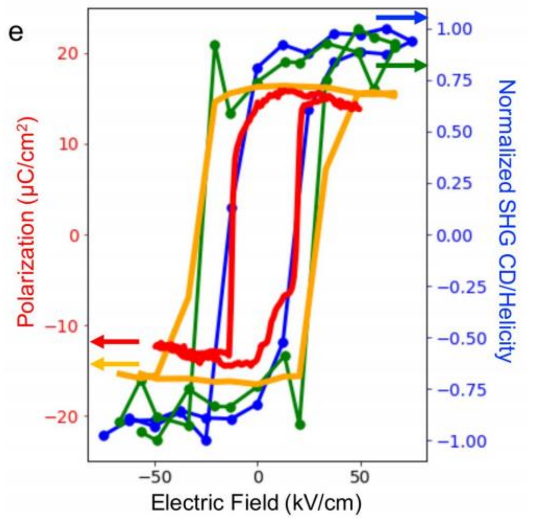

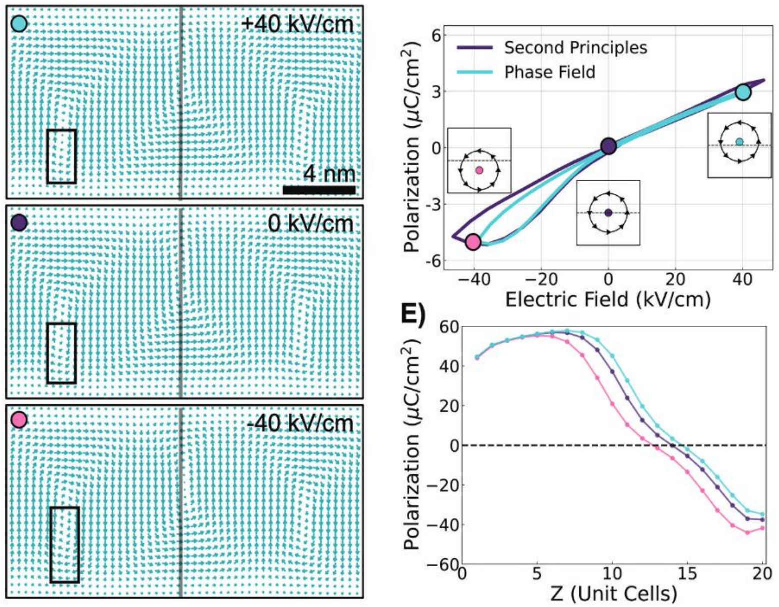

Tunable by means of electric or mechanical fields

S. Das,…, F. Gómez-Ortiz *et al.* Nature 568, 368 (2019)

P. Behera, F. Gómez Ortiz *et al*. Sci. Adv. **8**, eabj8030 (2022)

F. Gómez-Ortiz et al. arXiv:2401.13026 Accepted in Phys. Rev. Lett. (2024)